Supporting Information

A Novel Photo-Sulfite System: Towards Simultaneous Transformations of Inorganic and Organic Pollutants

Yaoguang Guo, Xiaoyi Lou, Changling Fang, Dongxue Xiao, Zhaohui Wang*, Jianshe Liu*

State Environmental Protection Engineering Center for Pollution Treatment and Control in Textile Industry, College of Environmental Science and Engineering, Donghua University, Shanghai, 201620, China

***Corresponding author: Zhaohui Wang, Jianshe Liu**

E-mail: zhaohuiwang@dhu.edu.cn (Z. Wang); liujianshe@dhu.edu.cn (J. Liu)

52 Figures

2 Tables

List of Supporting Information

degradation for 120 min in Fe(III)-S(IV) system.

Figure S8. The GC chromatograph of the sample after 2,4,6-TCP degradation for 30 min in photo-sulfite system.

Figure S9. The GC chromatograph of the silylated sample after 2,4,6-TCP degradation for 30 min in photo-sulfite system.

Figure S10. The GC chromatograph of the sample after 2,4,6-TCP degradation for 120 min in photo-sulfite system.

Figure S11. The GC chromatograph of the silylated sample after 2,4,6-TCP degradation for 120 min in photo-sulfite system.

Figure S12. The GC-MS spectrum of phenol.

Figure S13. The GC-MS spectrum of 2,6-dichlorophenol.

Figure S14. The GC-MS spectrum of 2,4,6-trichlorophenol.

Figure S15. The GC-MS spectrum of 2,3,4,6-tetrachlorophenol.

Figure S16. The GC-MS spectrum of trimethyl(phenoxy)silane.

Figure S17. The GC-MS spectrum of trimethyl(4-chlorophenoxy)silane.

Figure S18. The GC-MS spectrum of trimethyl(2,6-dichlorophenoxy)silane.

Figure S19. The GC-MS spectrum of trimethyl(2,4-dichlorophenoxy)silane.

Figure S20. The GC-MS spectrum of trimethyl(2,4,6-trichlorophenoxy)silane.

Figure S21. The GC-MS spectrum of trimethyl(2,3,4,6-tetrachlorophenoxy)silane.

Figure S22. The GC-MS spectrum of dibenzo[*b,d*]furan.

Figure S23. The GC-MS spectrum of trimethylsilyl hexanoate.

Figure S24. The GC-MS spectrum of bis(trimethylsilyl) oxalate.

Figure S25. Degradation of common aqueous organic pollutants in the novel photo-sulfite system.

Figure S26. S (IV) species distribution in Fe (III)-S(IV) system.

Figure S27. The effect of initial pH on the degradation of 2,4,6-TCP.

Figure S28. The degradation of 2,4,6-TCP under varying initial dosages ratio of S(IV): Fe(III) conditions.

Figure S29. The changes of pH during the degradation of 2,4,6-TCP in the UV-Fe(III)-S(IV) and Fe(III)-S(IV) systems.

Figure S30. The degradation of 2,4,6-TCP when UV irradiation introduction into Fe(III)-S(IV) after 60 min.

Figure S31. Fe(III) species distribution in Fe(III)-CH_3OONa-S(IV) system.

Figure S32. Acetate species distribution in Fe(III)-CH_3OONa-S(IV) system.

Figure S33. Fe(III) species distribution in Fe(III)-Ox-S(IV) system.

Figure S34. Oxalate species distribution in Fe(III)-Ox-S(IV)system.

Figure S35. Fe(III) species distribution in Fe(III)-Cit-S(IV) system.

Figure S36. Citrate species distribution in Fe(III)-Cit-S(IV) system.

Figure S37. Fe(III) species distribution in Fe (III)-EDTA-S(IV) system.

Figure S38. EDTA species distribution in Fe(III)-EDTA-S(IV) system.

Figure S39. The dosages of S(IV) after 2,4,6-TCP degradation for 30 min when Fe(III)-complexing ligands added into the photo-sulfite system.

Figure S40. Fe(III) species distribution in Fe (III)-NH_4F-S(IV) system.

Figure S41. F species distribution in Fe(III)-NH_4F-S(IV) system.

Figure S42. Fe (III) species distribution in Fe (III)-H_3PO_4-S(IV) system.

Figure S43. Phosphate species distribution in Fe(III)-H_3PO_4-S(IV) system.

Figure S44. The effect of Phen on the degradation of 2,4,6-TCP and the UV-visible spectrum of the degradation of 2,4,6-TCP after 120 min in different systems.

Figure S45. Decoloration of MO under varying experimental conditions.

Figure S46. The degradation of MO under varying initial dosages ratio of S(IV): Fe(III) conditions in the photo-sulfite system.

Figure S47. The changes of pH during the degradation of MO in the UV-Fe(III)-S(IV) and Fe(III)-S(IV) systems.

Figure S48. The variations of Fe(II) concentration, S(IV) conversion, Fe speciation during the MO degradation in Fe(III)-S(IV) and UV-Fe(III)-S(IV) systems.

Figure S49. The decoloration of MO when UV irradiation introduction into Fe(III)-S(IV) after 60 min.

Figure S50. The effects of Fe(III) complexation on the decoloration of MO.

Figure S51. The dosages of S(IV) after MO degradation for 30 min when Fe(III)-complexing ligands added into the photo-sulfite system.

Figure S52. Degradation of 2,4,6-TCP in the photo-sulfite and UV/persulfate systems.

Table S1. The common information of the selected substrates

Name	CAS Number	Formula	Structure	Max absorption wavelength (nm)
Methyl Orange	547-58-0	$C_{14}H_{14}N_3NaO_3S$	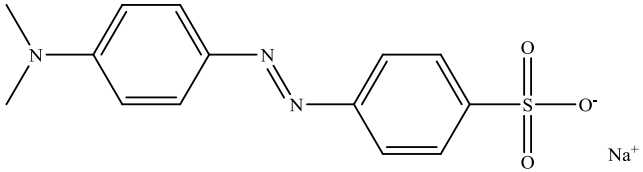	487[a]
Acid Orange 7	633-96-5	$C_{16}H_{11}N_2NaO_4S$	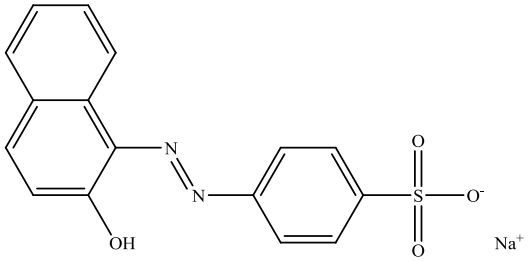	484[a]
Methylene Blue	7220-79-3	$C_{16}H_{18}ClN_3S\cdot3H_2O$	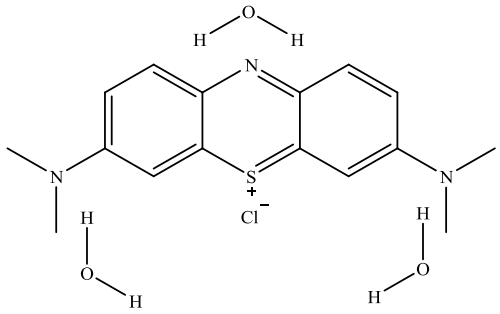	663[a]

Rhodamine B	81-88-9	$C_{28}H_{31}ClN_2O_3$	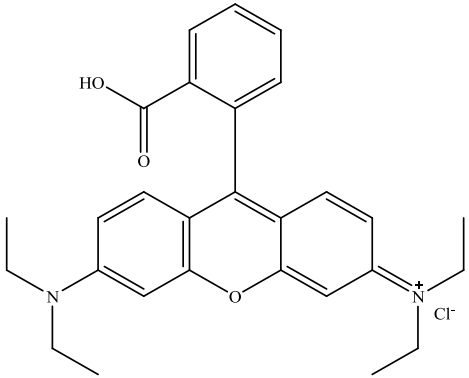	554[a]
2,4,6-trichlorophenol	1988-6-2	$C_6H_3Cl_3O$	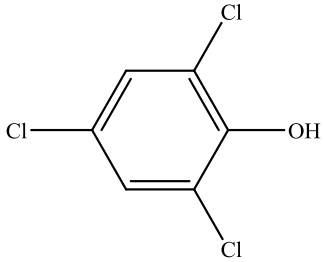	290[b]

[a] The Max absorption wavelength of the selected dyes determined via wavelength scan mode in a Hitachi U-2910 spectrophotometer.

[b] The wavelength used to analyze the concentration of 2,4,6- trichlorophenol by HPLC equipped with UV-vis detector .

Table S2. Spectrum distribution and relative energy of medium-pressure Hg lamp

Wavelength (nm)	265.2-265.5	296.7	302.2-302.8	312.6-313.2	365.0-366.3	404.5-407.8	435.8	546.1	577.0-579.0
Relative energy (%)	15.3	16.6	23.9	49.9	100	42.2	77.5	93	76.5

The detailed preparation of all selected solutions

0.05 g Ferric sulfate ($Fe_2(SO_4)_3$, AR) was added into 50 mL volumetric flask filled with acidic solution of pH = 4.0 adjusted with NaOH and H_2SO_4 to prepare stock solutions of $Fe_2(SO_4)_3$ with the concentration of 2.5 mM, followed by adjusting pH = 4.00 ± 0.05 with NaOH and H_2SO_4 as quickly as possible. The sulfite stock solutions with the concentration of 50 mM were prepared by adding 0.63 g anhydrous sodium sulfite (Na_2SO_3, AR) into 100 mL volumetric flask filled with acidic solution of pH = 4.0 adjusted with NaOH and H_2SO_4, followed by adjusting pH = 4.00 ± 0.05 with NaOH and H_2SO_4 as quickly as possible, which were used as air-saturated solutions in order to avoid any loss in sulfur(IV) concentration by both oxidation and emission of SO_2. The stock solutions of other substrates were prepared by adding the desired amounts to the acidic solution of pH = 4.0 adjusted with NaOH and H_2SO_4, followed by adjusting pH = 4.00 ± 0.05 with NaOH and H_2SO_4 as quickly as possible. All stock solutions were prepared freshly each time.

Substrates at desired concentrations were spiked in an open cylindrical glass tube with 50 mL capacity under magnetic stirring with a PTFE-coated magnetic stirrer at an initial pH of 4.00 ± 0.05 (adjusted with NaOH and H_2SO_4). Then Fe (III) was added at the desired concentration. Each run was switched on by the careful addition of the desired concentration of Na_2SO_3. During the remaining reaction process, the pH was not controlled.

GC-MS analyses

Intermediate compounds during 2,4,6-TCP degradation process were identified using GC-MS. Samples were pretreated by liquid-liquid extraction (using CH_2Cl_2 solvent) and silylation method (using hexamethyldisilazane and chlorotrimethylsilane) to extract and concentrate compounds of different polarity and volatility. Spectra were obtained with a GC (Agilent 7890A), equipped with HB-5 MS capillary column (30 m × 320 μm × 0.5 μm film thickness), interfaced directly to the mass spectrometer (5975A inert XL MSD with Triple-Axis Detector) used as a detector. The injections were made in the splitless mode using an injection temperature of 250℃. Helium was used as carrier gas. The GC column was operated in a temperature programmed mode with an initial temperature of 40℃ held for 5min, ramp first to 100℃ with a 15℃ /min rate, then to 200℃ with 5℃/min rate, and then to 270℃ with 20 ℃/min rate and held at that temperature for 5 min. Mass spectra were recorded in electron ionization (EI) mode at an ion source temperature of 230℃ and electron energy of 70eV. The mass range scanned was 30-400m/z. The substance analysis was undertaken with reference to the NIST08 mass spectral library database.

Silylation method

The sample after extractive treatment was firstly was dried under a gentle nitrogen stream. The dry material was then treated with 0.4 mL of anhydrous pyridine, 0.2 mL of hexamethyldisilazane, and 0.1 mL of chlorotrimethylsilane. The reaction was carried out in a 2 mL plastic-stoppered vial. The mixture was shaken vigorously for about 60 s and then allowed to stand for 5 min at room temperature. Precipitate was separated by centrifugation for 2 min ($r = 1.2 \times 10^4$ r/min) prior to chromatographic analysis.

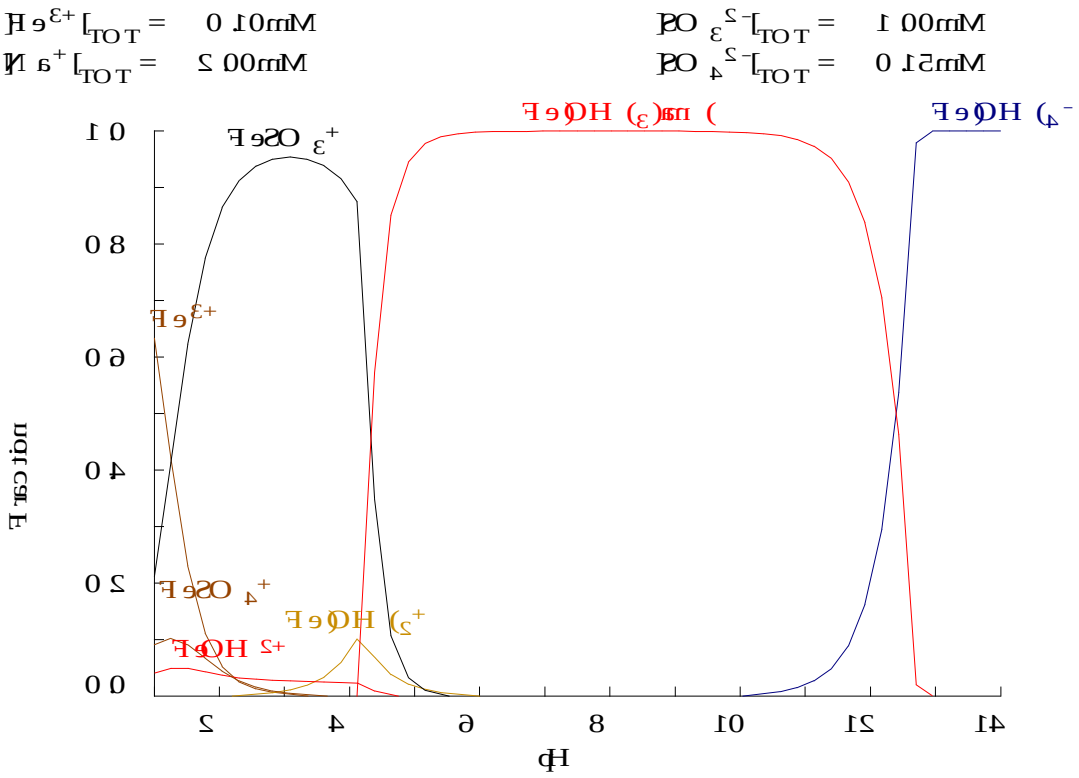

Figure S1. Fe (III) species distribution in Fe (III)-S(IV) system.

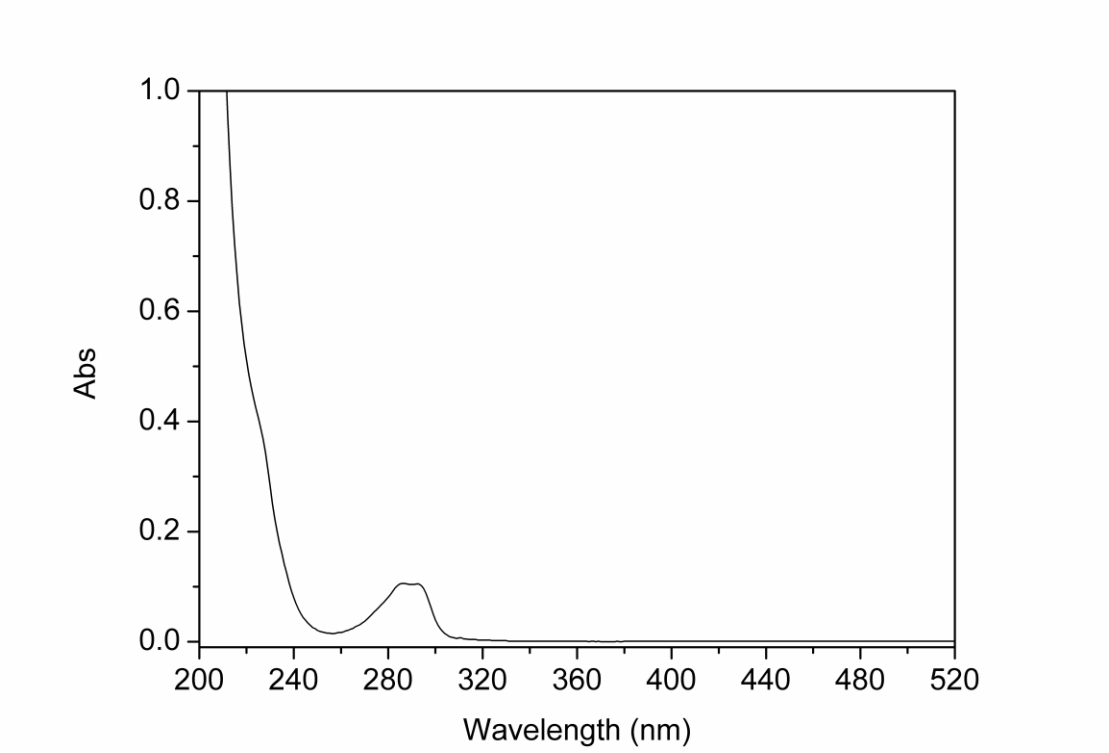

Figure S2. UV-visible adsorption spectrum of 10mg/L of 2,4,6-TCP within the wavelength from 200 nm to 520 nm.

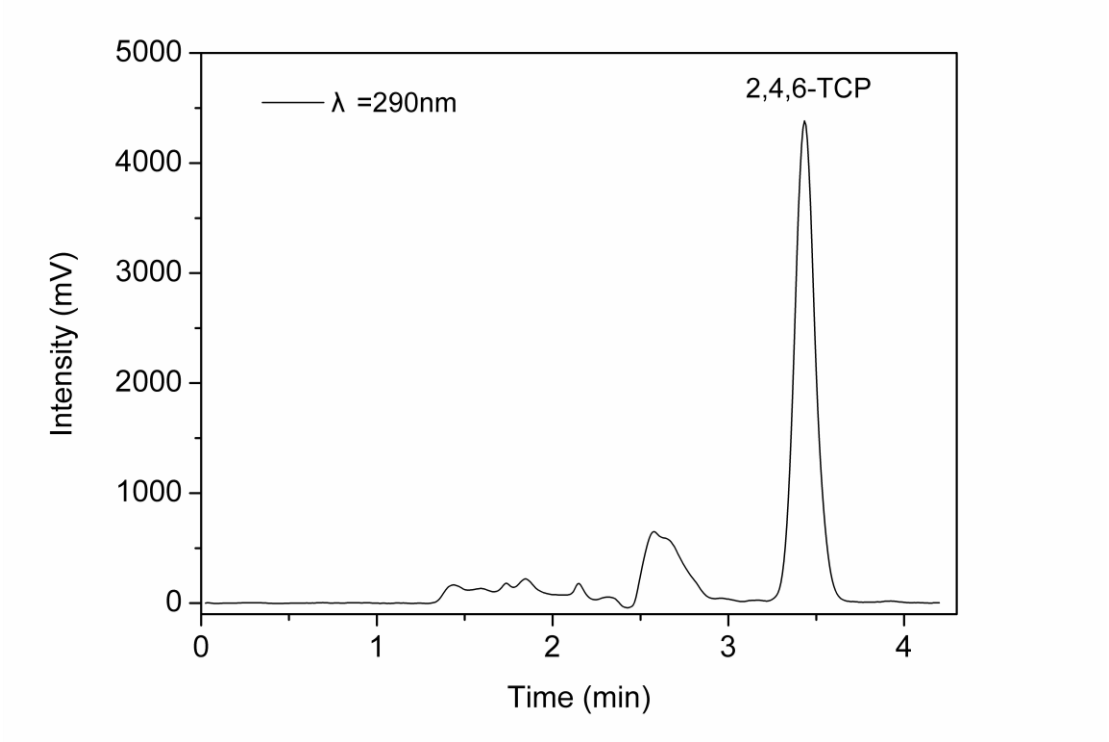

Figure S3. The HPLC chromatogram map of 2,4,6-TCP. Conditions: $[2,4,6\text{-TCP}]_0$ = 10mg/L, Athena C18 column (4.6 mm × 250 mm, 5 μm) maintained at 30℃, the wavelength (λ) was 290 nm, the mobile phase was methanol/water = 85/15 (v/v), the flow rate was1.2 mL/min.

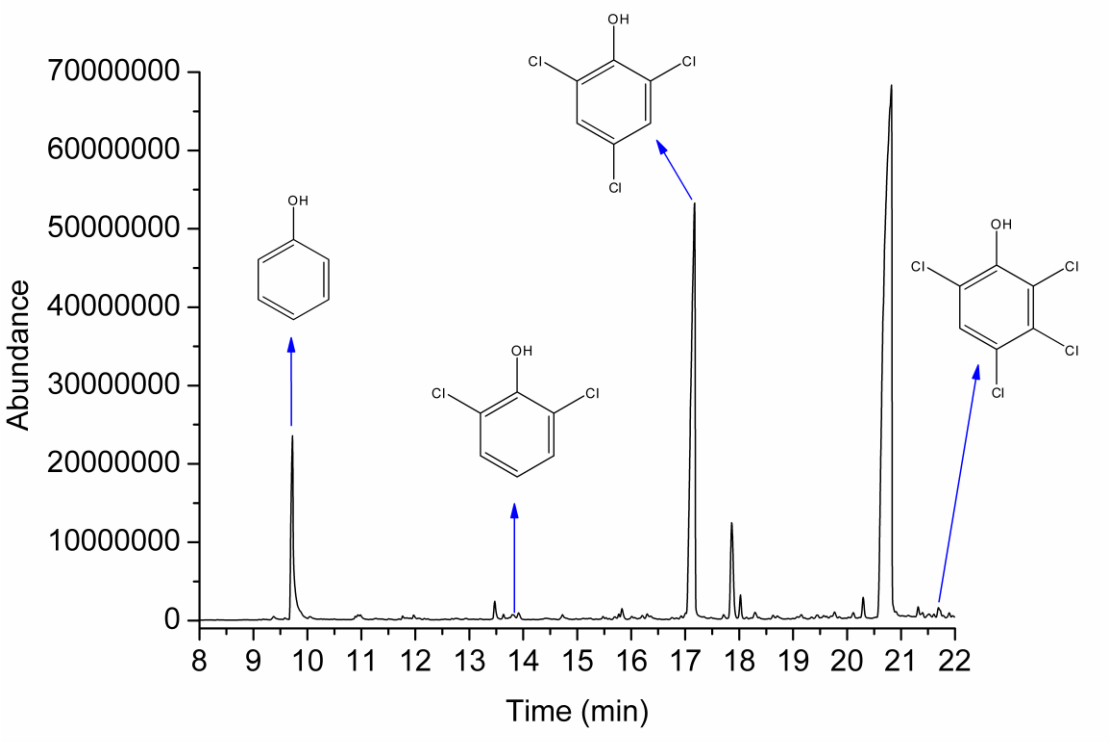

Figure S4. The GC chromatograph of the sample after 2,4,6-TCP degradation for 30 min in Fe(III)-S(IV) system.

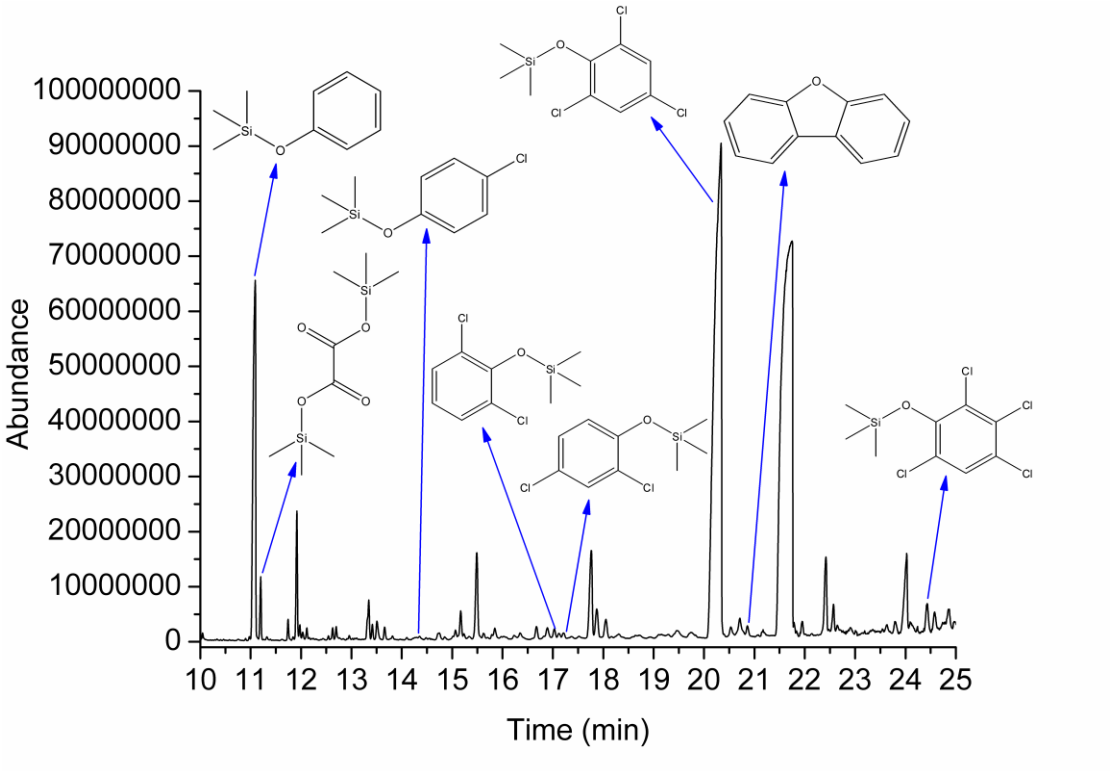

Figure S5. The GC chromatograph of the silylated sample after 2,4,6-TCP degradation for 30 min in Fe(III)-S(IV) system.

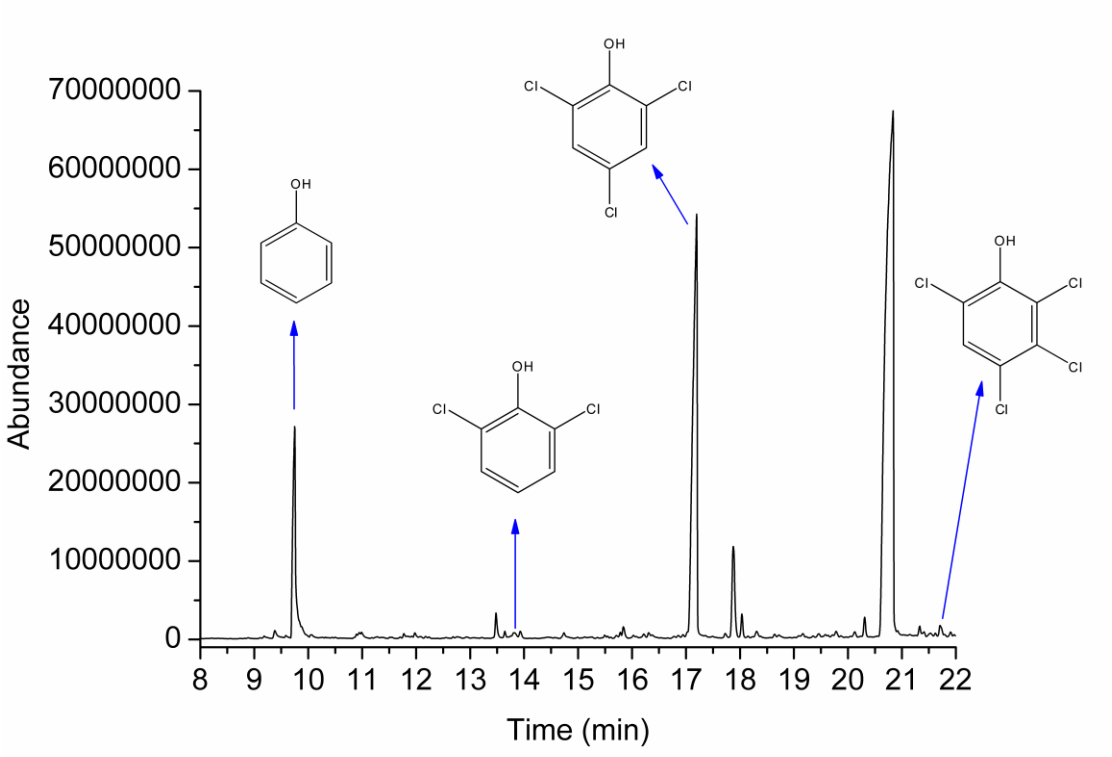

Figure S6. The GC chromatograph of the sample after 2,4,6-TCP degradation for 120 min in Fe(III)-S(IV) system.

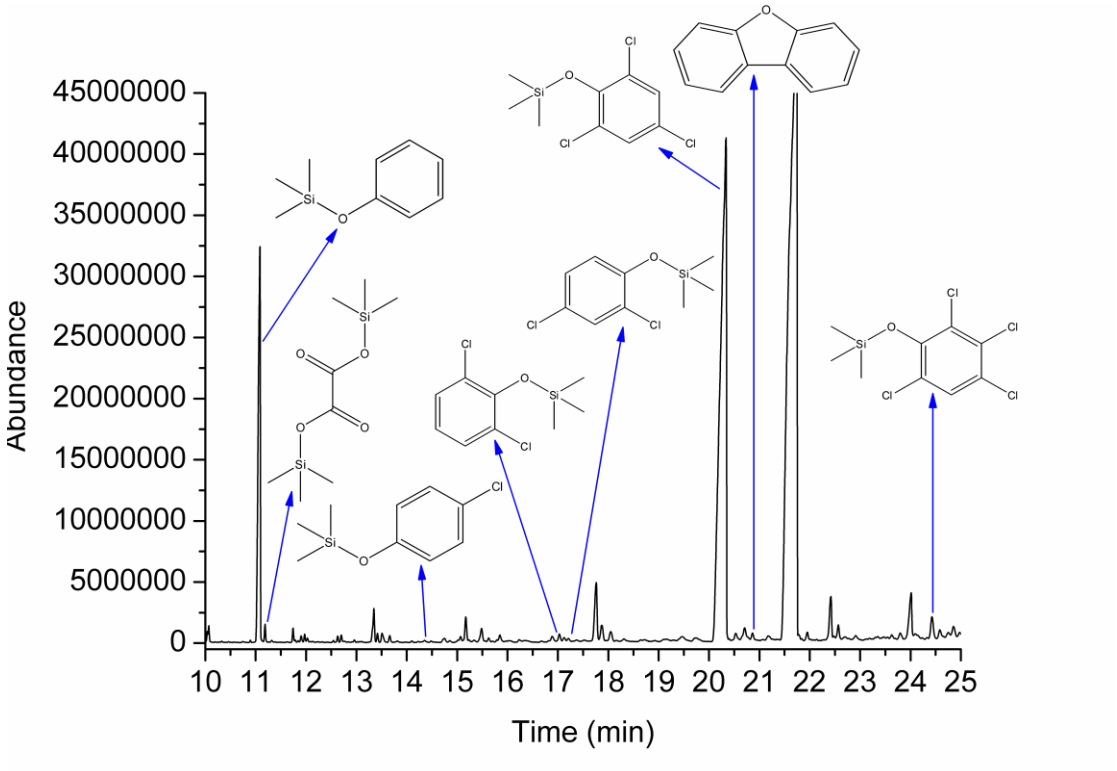

Figure S7. The GC chromatograph of the silylated sample after 2,4,6-TCP degradation for 120 min in Fe(III)-S(IV) system.

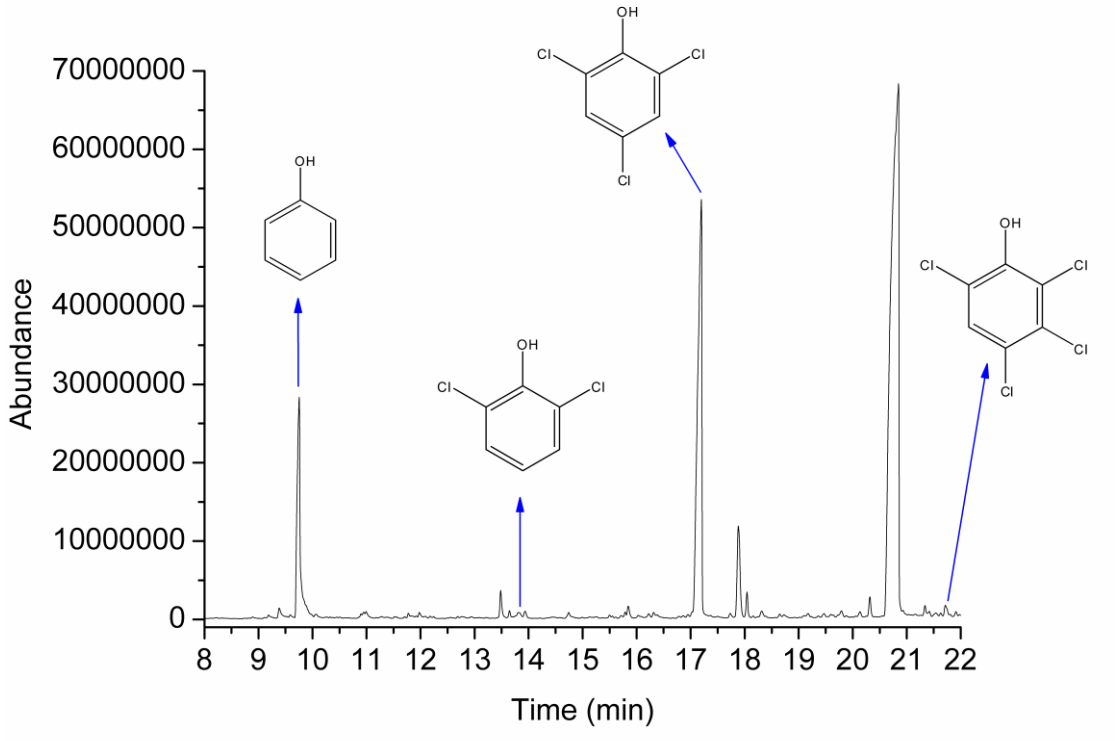

Figure S8. The GC chromatograph of the sample after 2,4,6-TCP degradation for 30 min in photo-sulfite system.

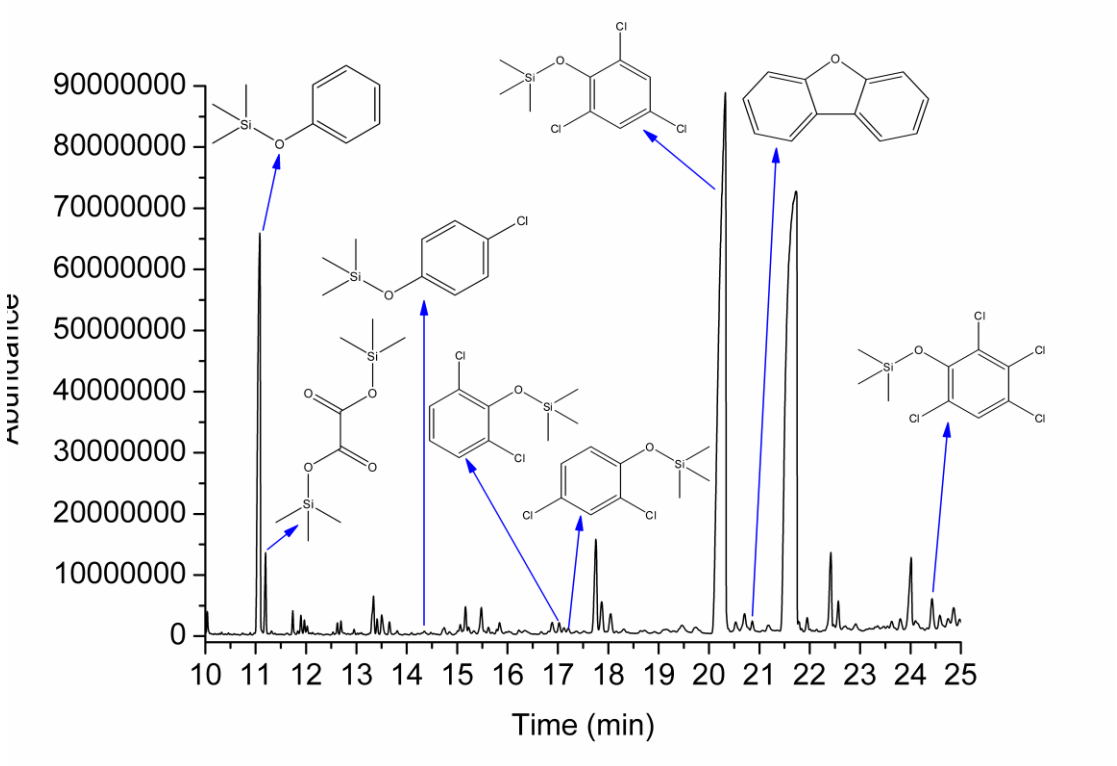

Figure S9. The GC chromatograph of the silylated sample after 2,4,6-TCP degradation for 30 min in photo-sulfite system.

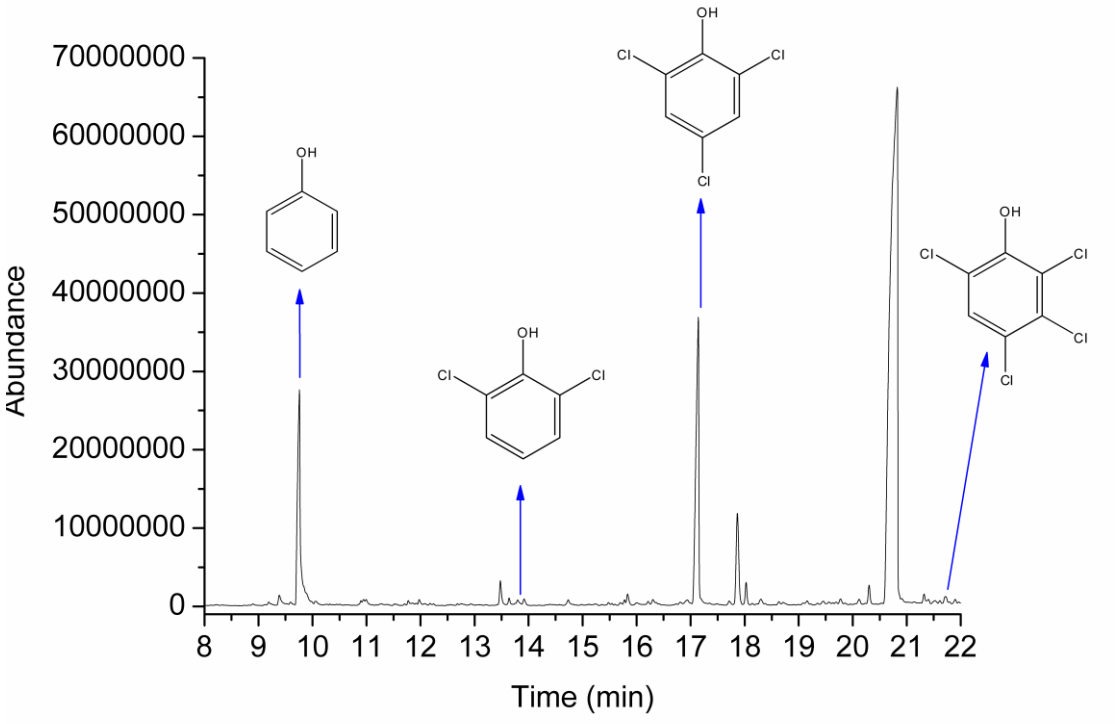

Figure S10. The GC chromatograph of the sample after 2,4,6-TCP degradation for 120 min in photo-sulfite system.

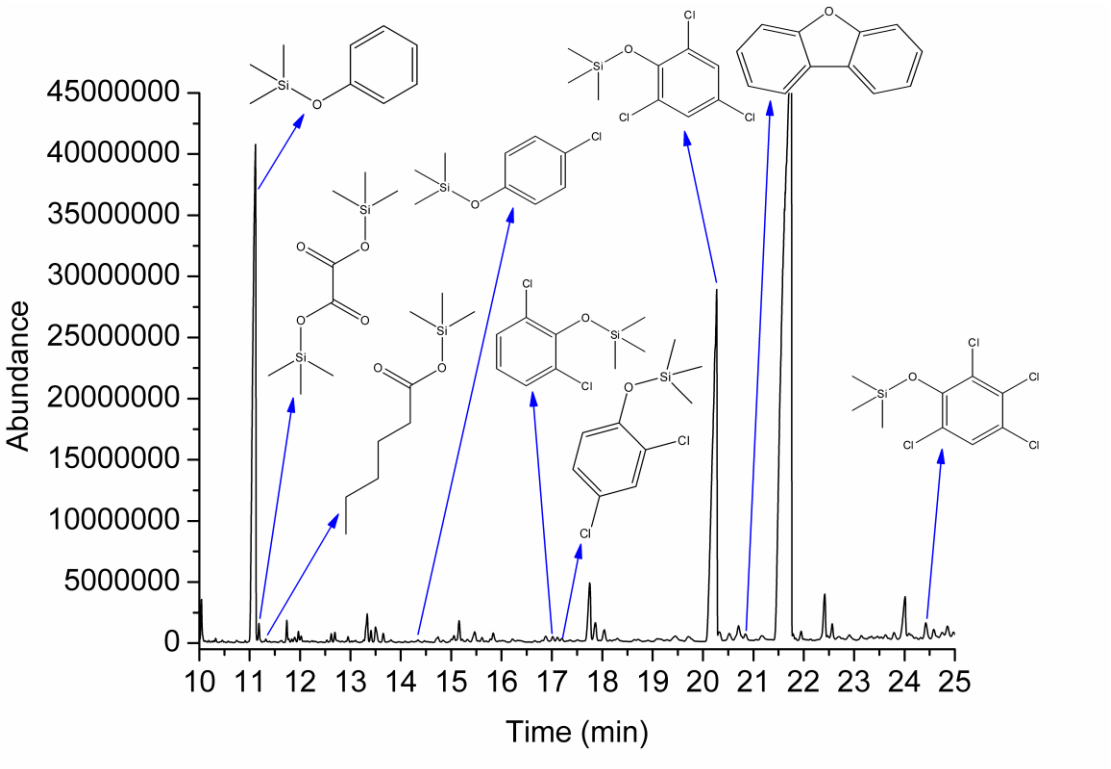

Figure S11. The GC chromatograph of the silylated sample after 2,4,6-TCP degradation for 120 min in photo-sulfite system.

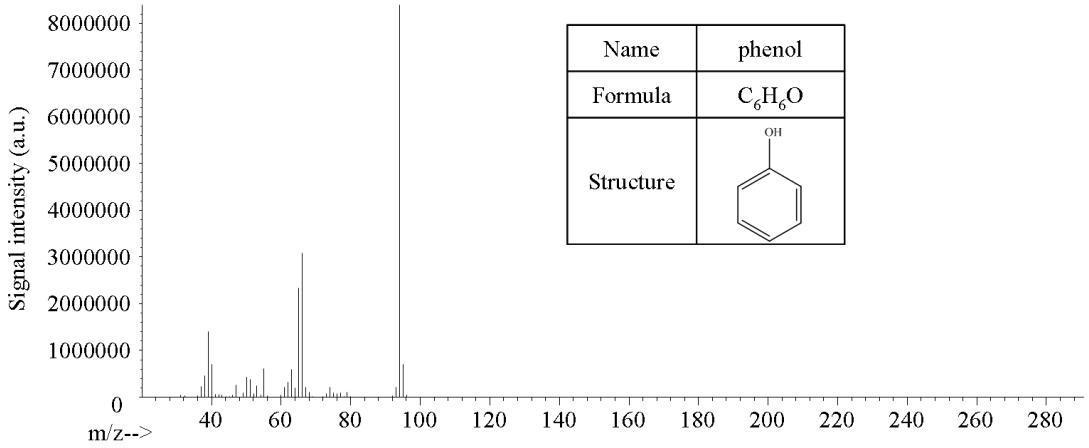

Figure S12. The GC-MS spectrum of phenol.

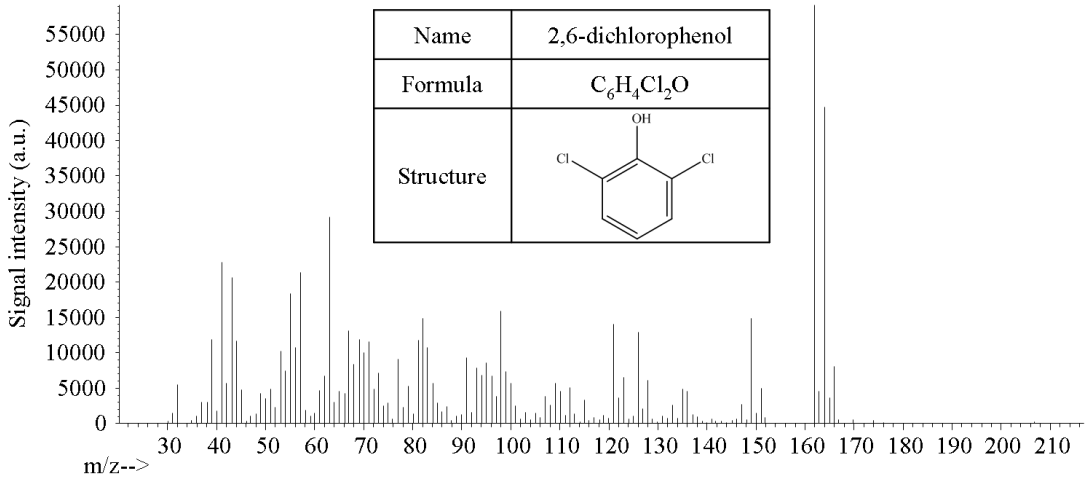

Figure S13. The GC-MS spectrum of 2,6-dichlorophenol.

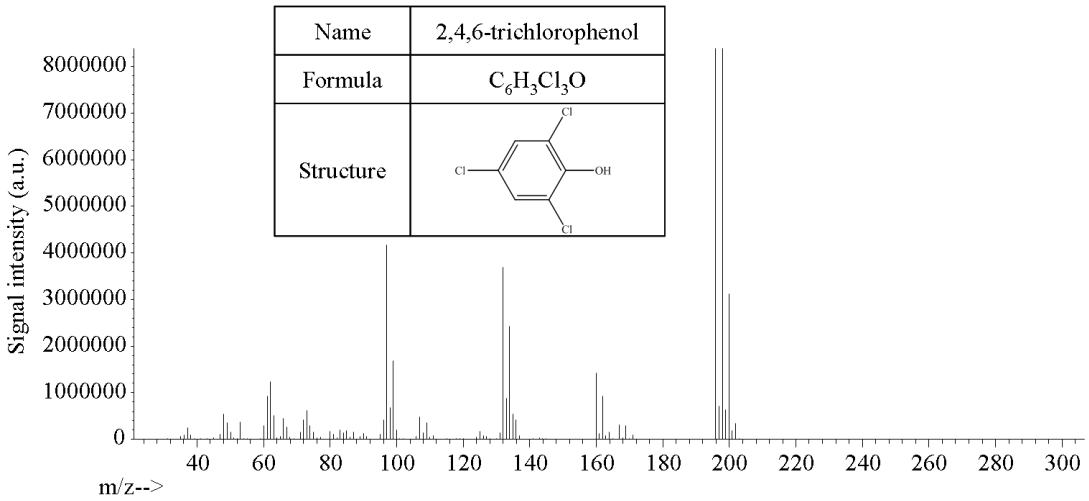

Figure S14. The GC-MS spectrum of 2,4,6-trichlorophenol.

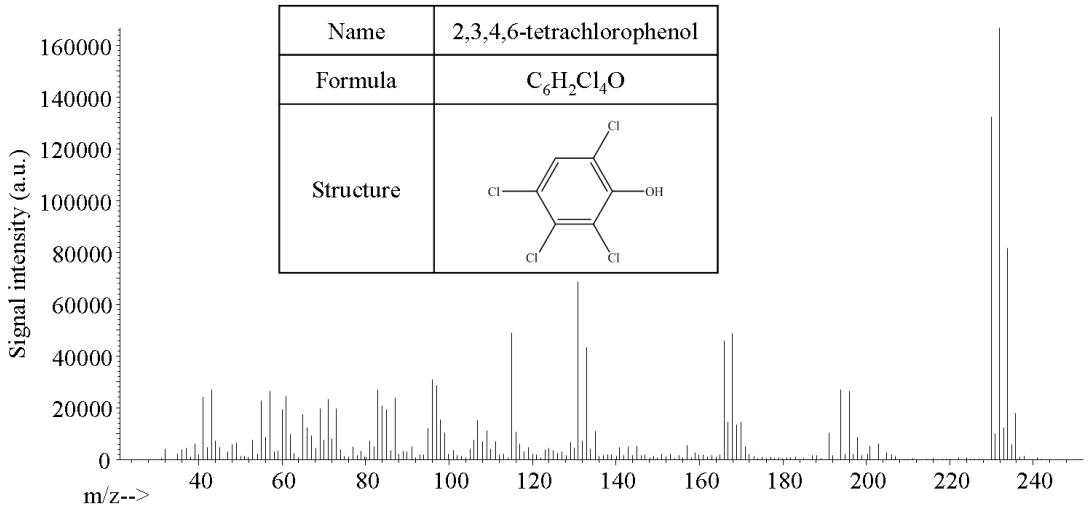

Figure S15. The GC-MS spectrum of 2,3,4,6-tetrachlorophenol.

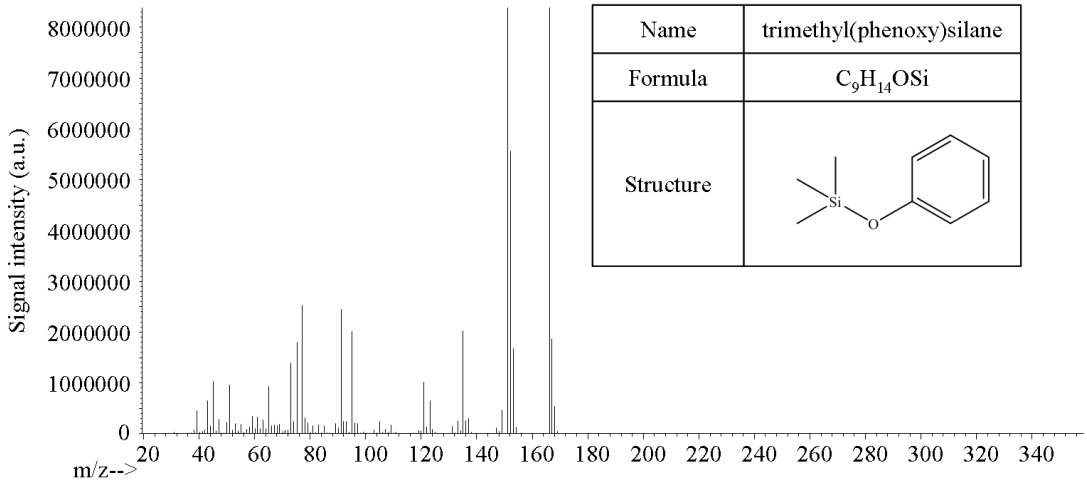

Figure S16. The GC-MS spectrum of trimethyl(phenoxy)silane.

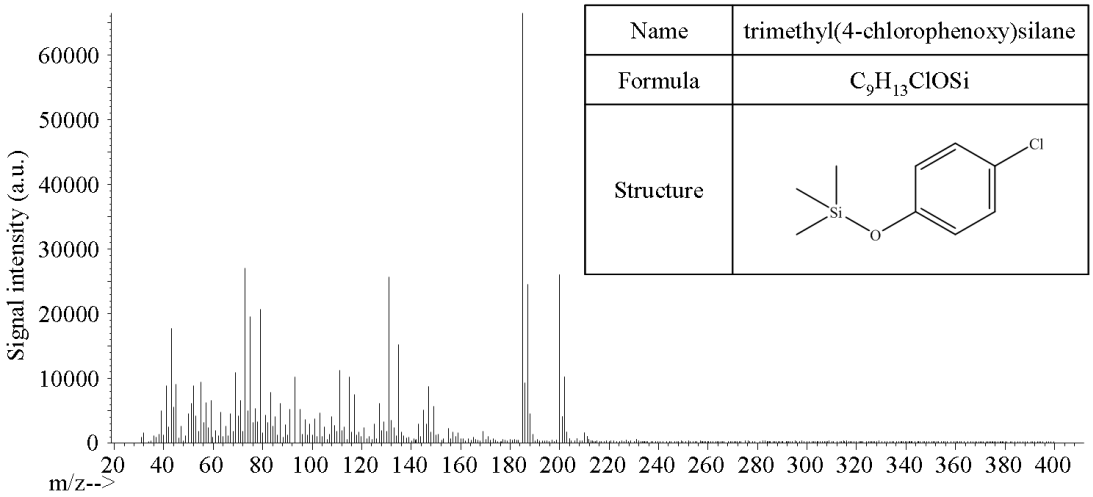

Figure S17. The GC-MS spectrum of trimethyl(4-chlorophenoxy)silane.

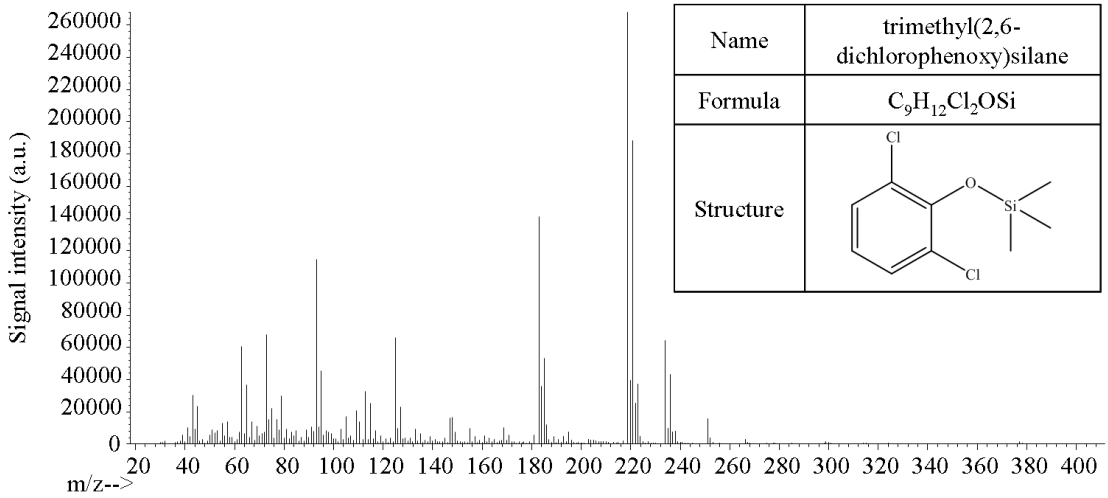

Figure S18. The GC-MS spectrum of trimethyl(2,6-dichlorophenoxy)silane.

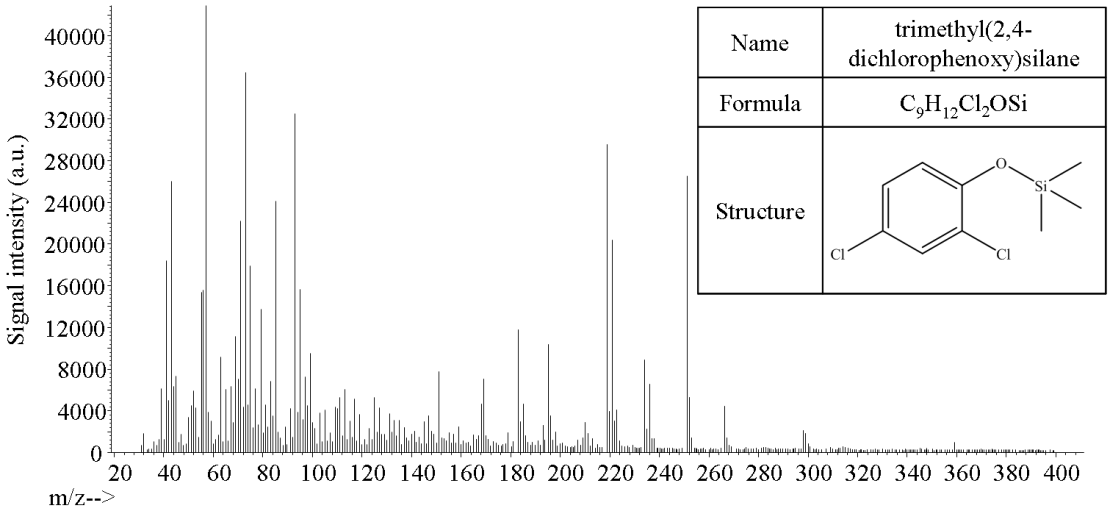

Figure S19. The GC-MS spectrum of trimethyl(2,4-dichlorophenoxy)silane.

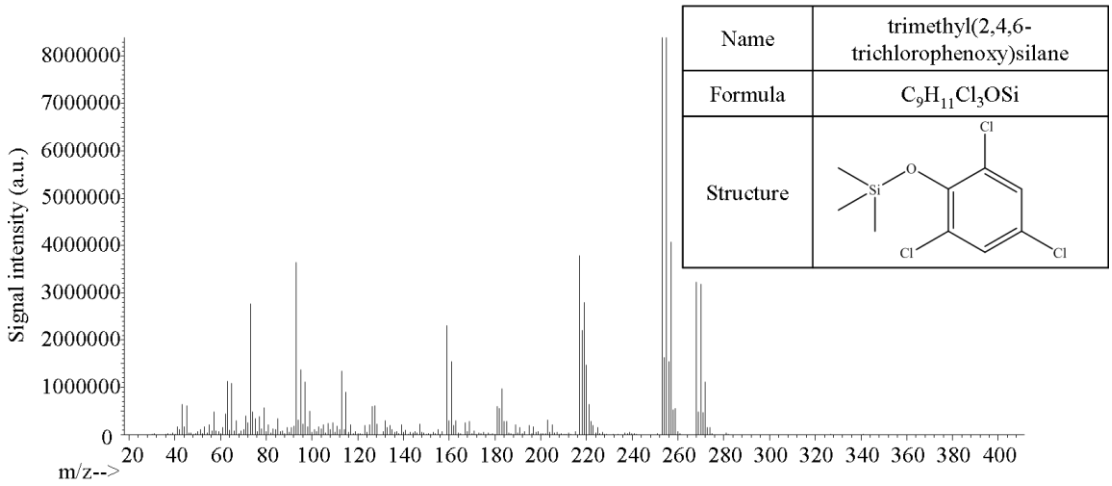

Figure S20. The GC-MS spectrum of trimethyl(2,4,6-trichlorophenoxy)silane.

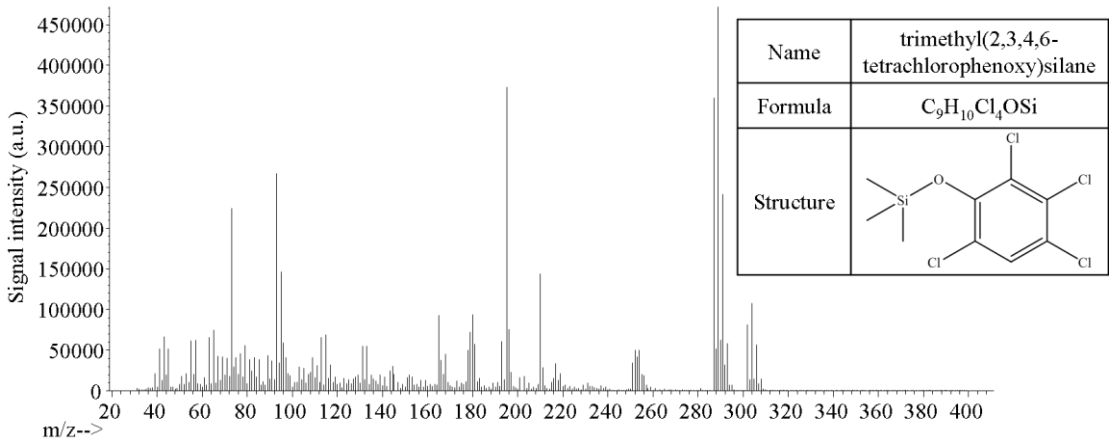

Figure S21. The GC-MS spectrum of trimethyl(2,3,4,6-tetrachlorophenoxy)silane.

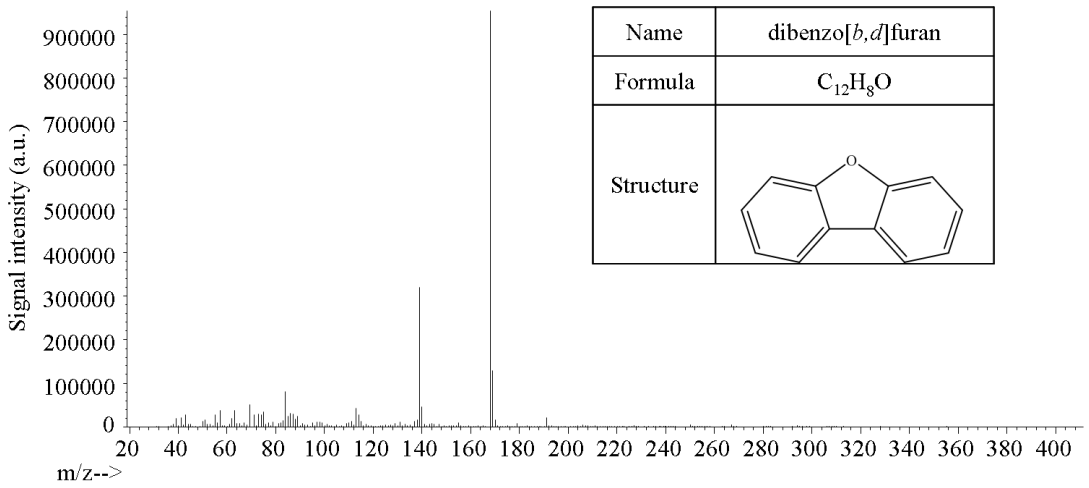

Figure S22. The GC-MS spectrum of dibenzo[*b*,*d*]furan.

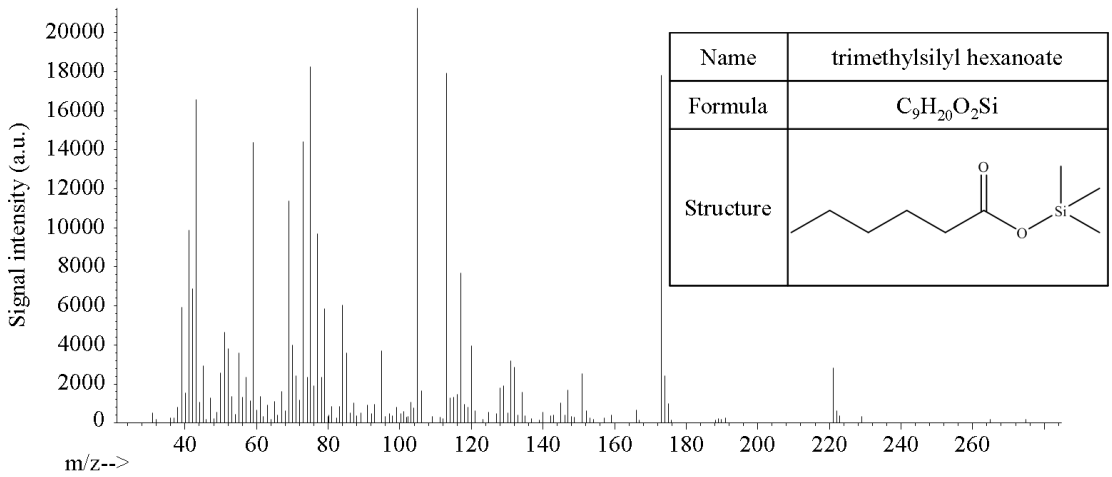

Figure S23. The GC-MS spectrum of trimethylsilyl hexanoate.

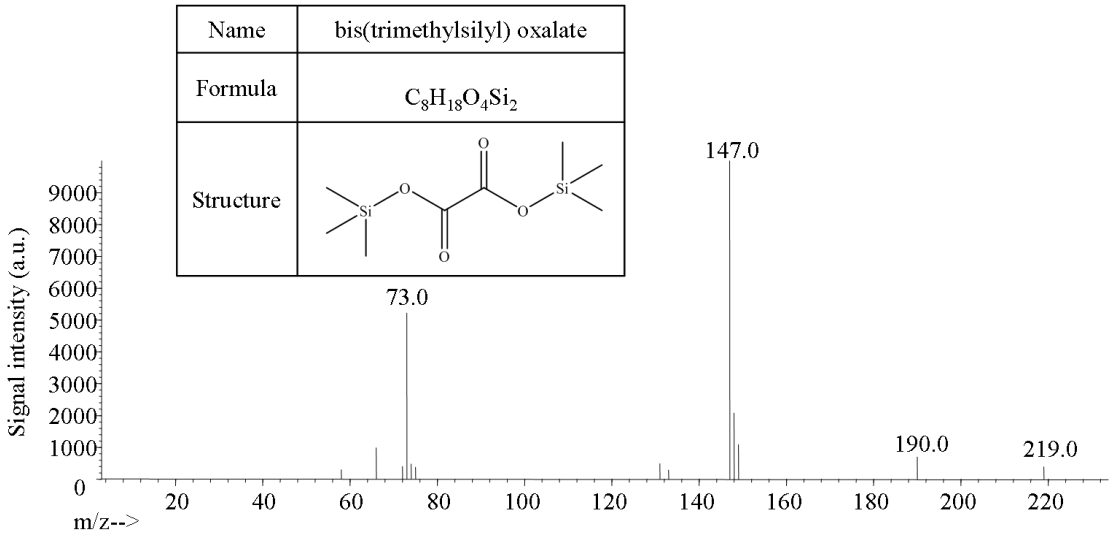

Figure S24. The GC-MS spectrum of bis(trimethylsilyl) oxalate.

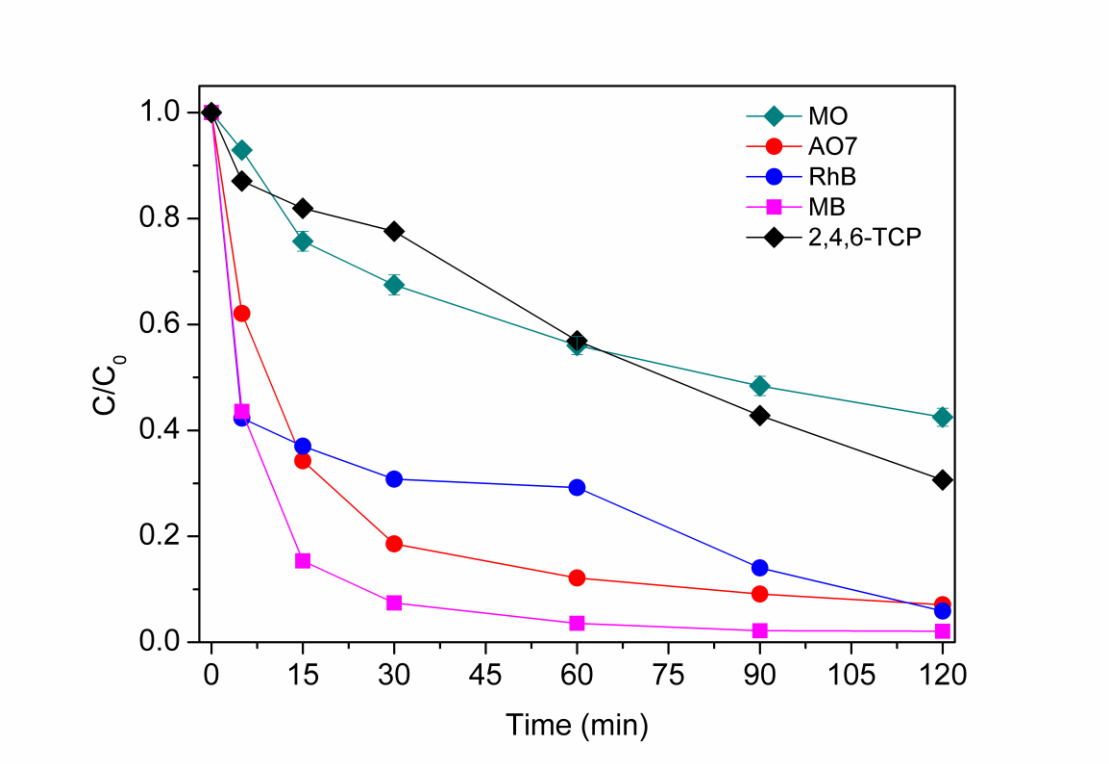

Figure S25. Degradation of common aqueous organic pollutants in the novel photo-sulfite system. Conditions: $[MO]_0 = [AO7]_0 = [2,4,6\text{-TCP}]_0 = 10$ mg/L, $[RhB]_0 = [MB]_0 = 5$ mg/L, $[Fe_2(SO_4)_3]_0 = 0.05$ mM, $[Na_2SO_3]_0 = 1$ mM, $pH_{ini} = 4$.

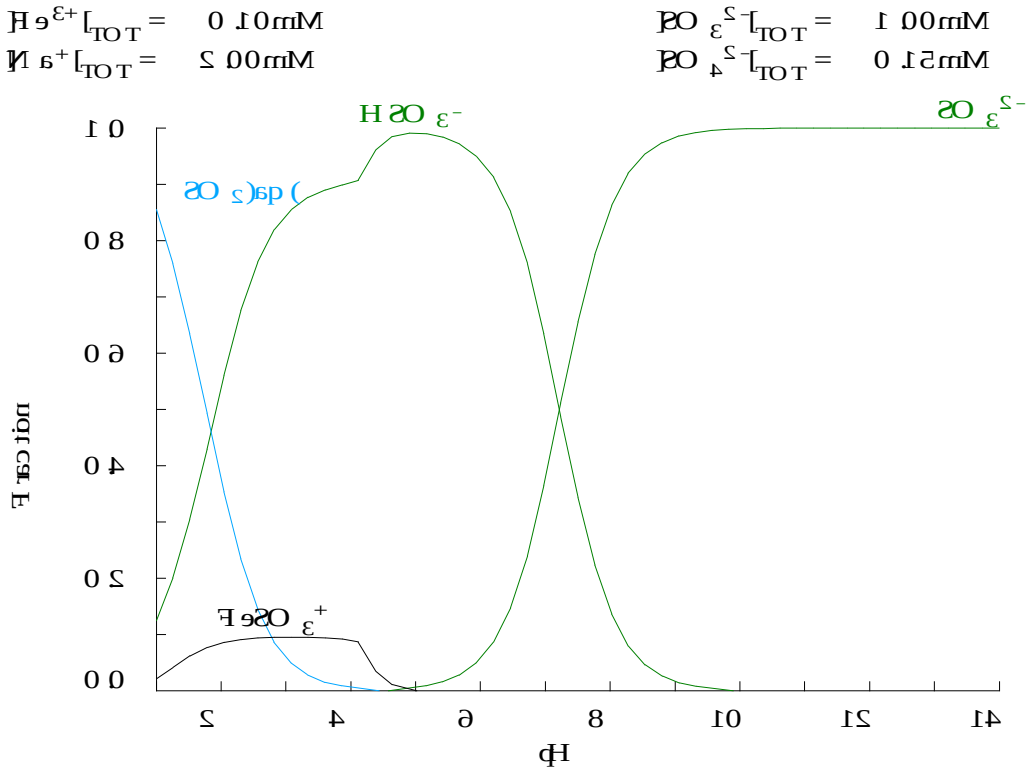

Figure S26. S (IV) species distribution in Fe (III)-S(IV) system.

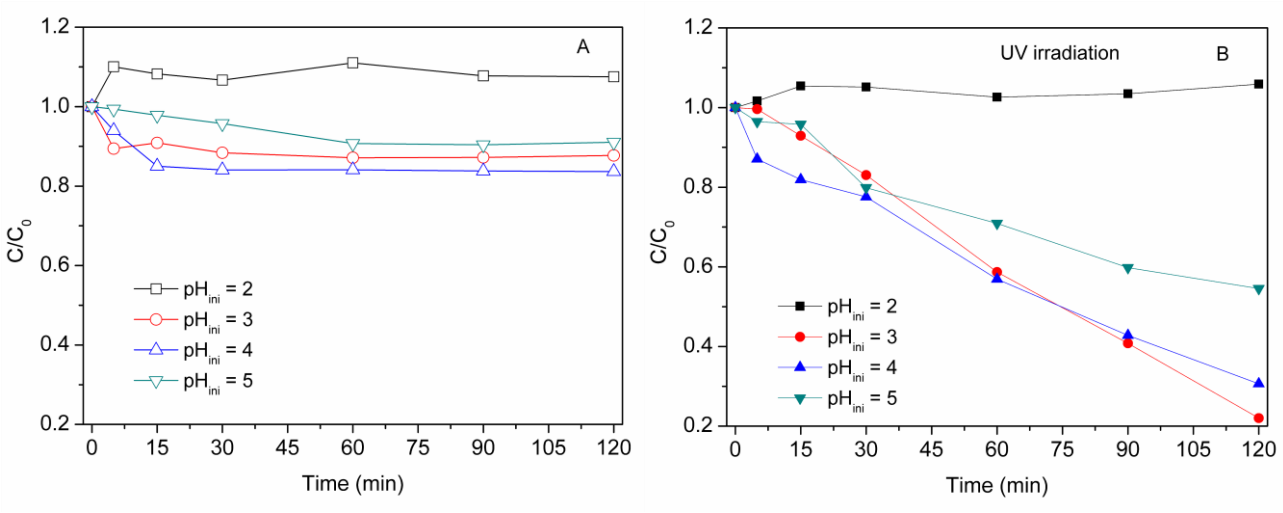

Figure S27. The effect of initial pH on the degradation of 2,4,6-TCP. Conditions: $[2,4,6\text{-TCP}]_0$ = 10 mg/L, $[Fe_2(SO_4)_3]_0$ = 0.05 mM, $[Na_2SO_3]_0$ = 1 mM.

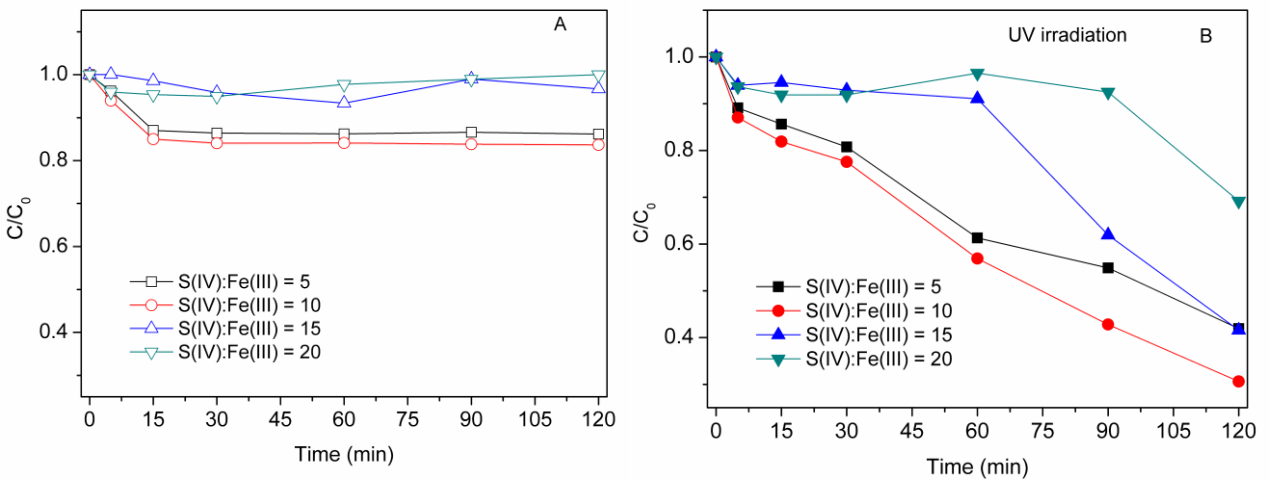

Figure S28. The degradation of 2,4,6-TCP under varying initial dosages ratio of S(IV): Fe (III) conditions. Conditions: $[2,4,6\text{-TCP}]_0$ = 10 mg/L, $[Fe_2(SO_4)_3]_0$ = 0.05 mM , pH_{ini} = 4.

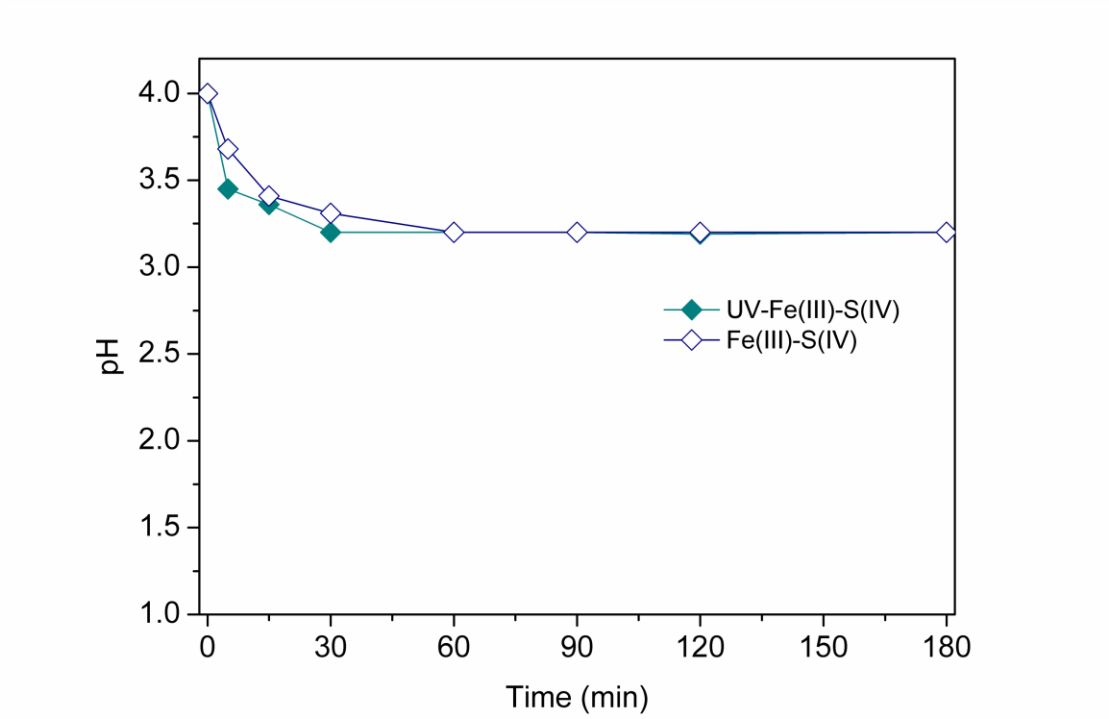

Figure S29. The changes of pH during the degradation of 2,4,6-TCP in the UV-Fe(III)-S(IV) and Fe(III)-S(IV) systems. Conditions: $[2,4,6\text{-TCP}]_0$ = 10 mg/L, $[Fe_2(SO_4)_3]_0$ = 0.05 mM, $[Na_2SO_3]_0$ = 1 mM, pH_{ini} = 4.

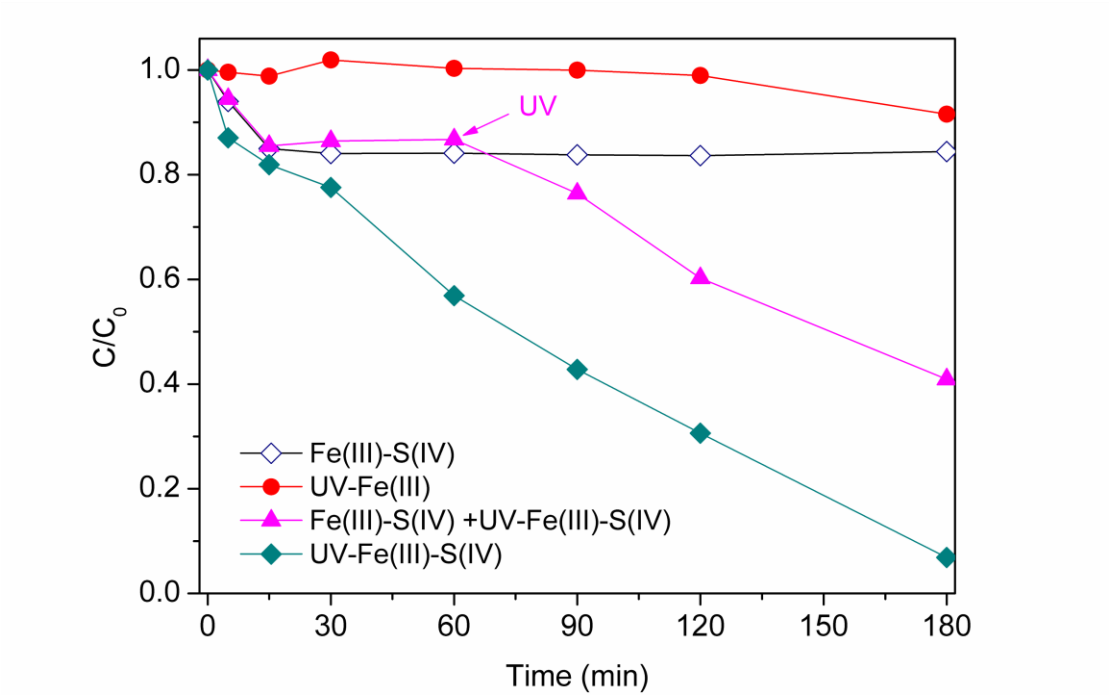

Figure S30. The degradation of 2,4,6-TCP when UV irradiation introduction into Fe (III)-S(IV) after 60 min. Conditions: $[2,4,6\text{-TCP}]_0$ = 10 mg/L, $[Fe_2(SO_4)_3]_0$ = 0.05 mM, $[Na_2SO_3]_0$ = 1 mM, pH_{ini} = 4.

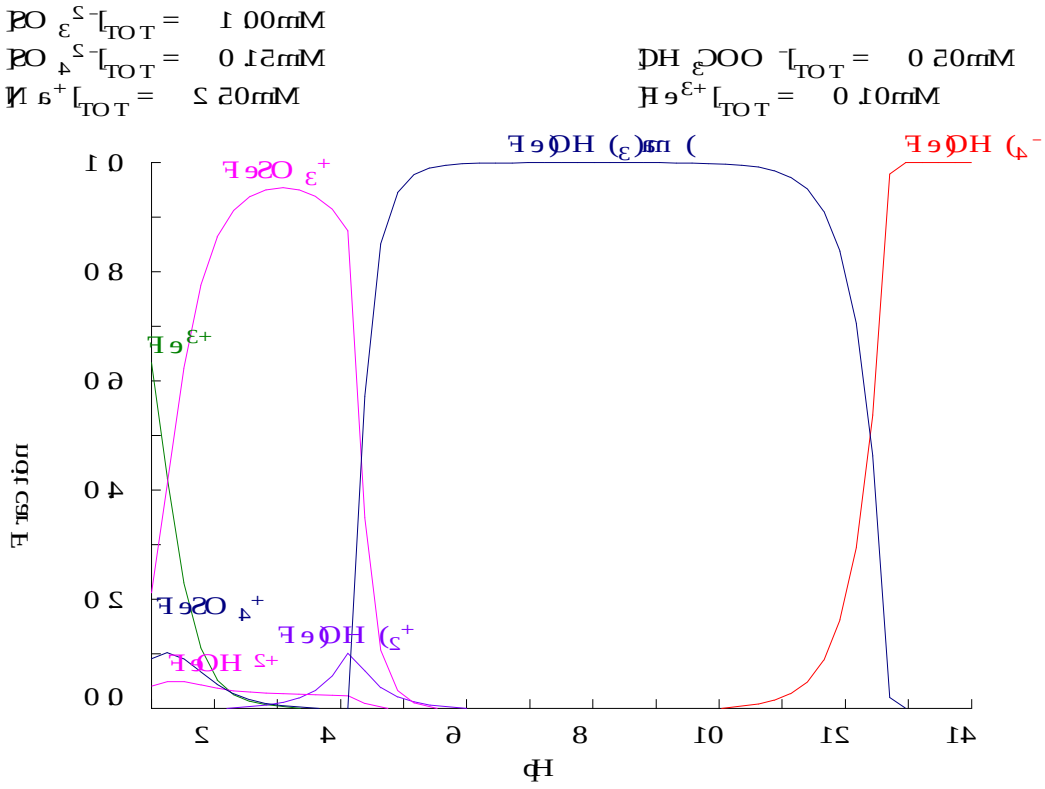

Figure S31. Fe(III) species distribution in Fe(III)-CH_3OONa-S(IV) system.

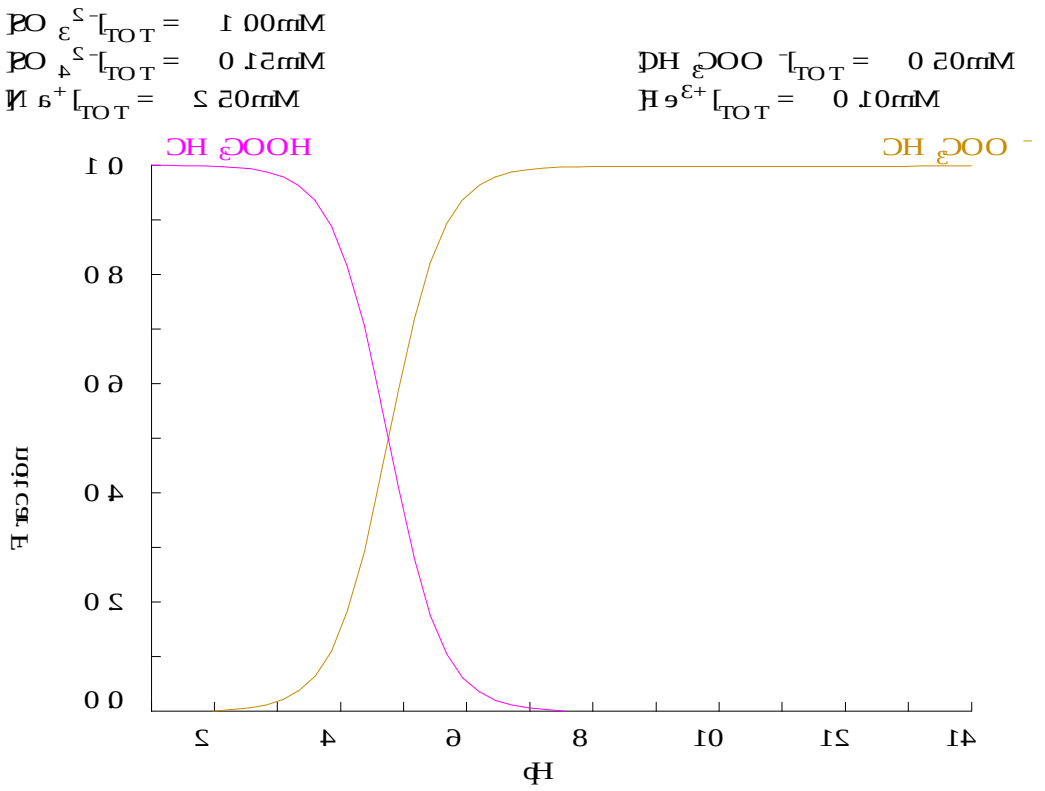

Figure S32. Acetate species distribution in Fe(III)-CH_3OONa-S(IV) system.

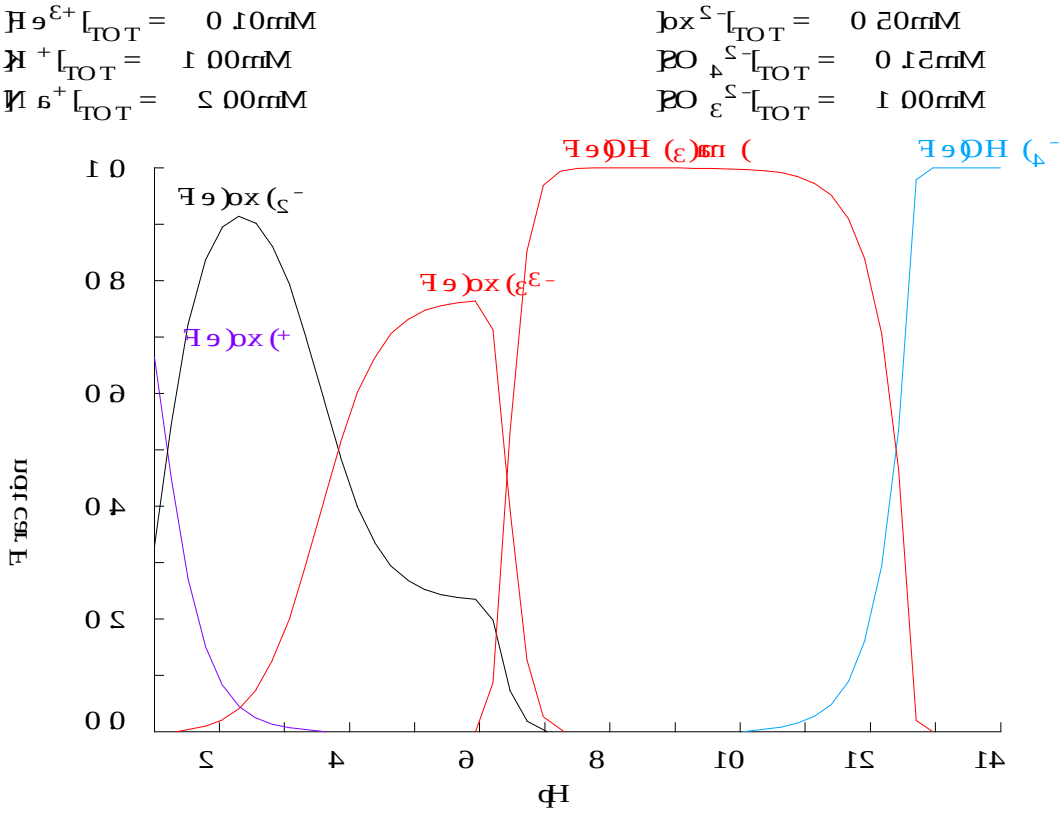

Figure S33. Fe(III) species distribution in Fe(III)-Ox-S(IV) system.

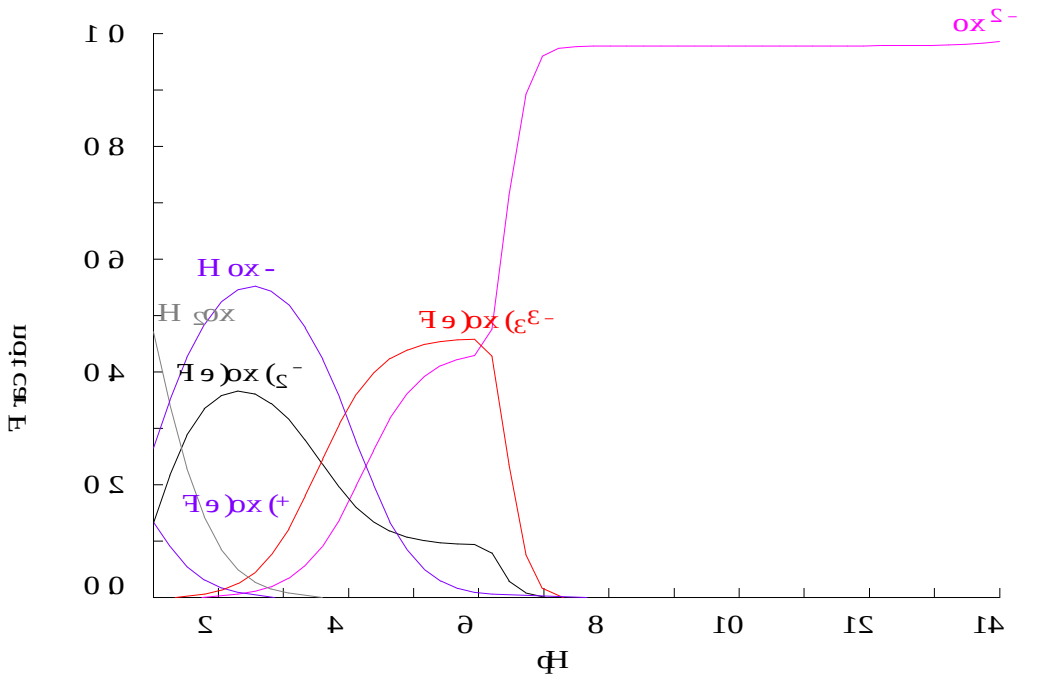

Figure S34. Oxalate species distribution in Fe(III)-Ox-S(IV)system.

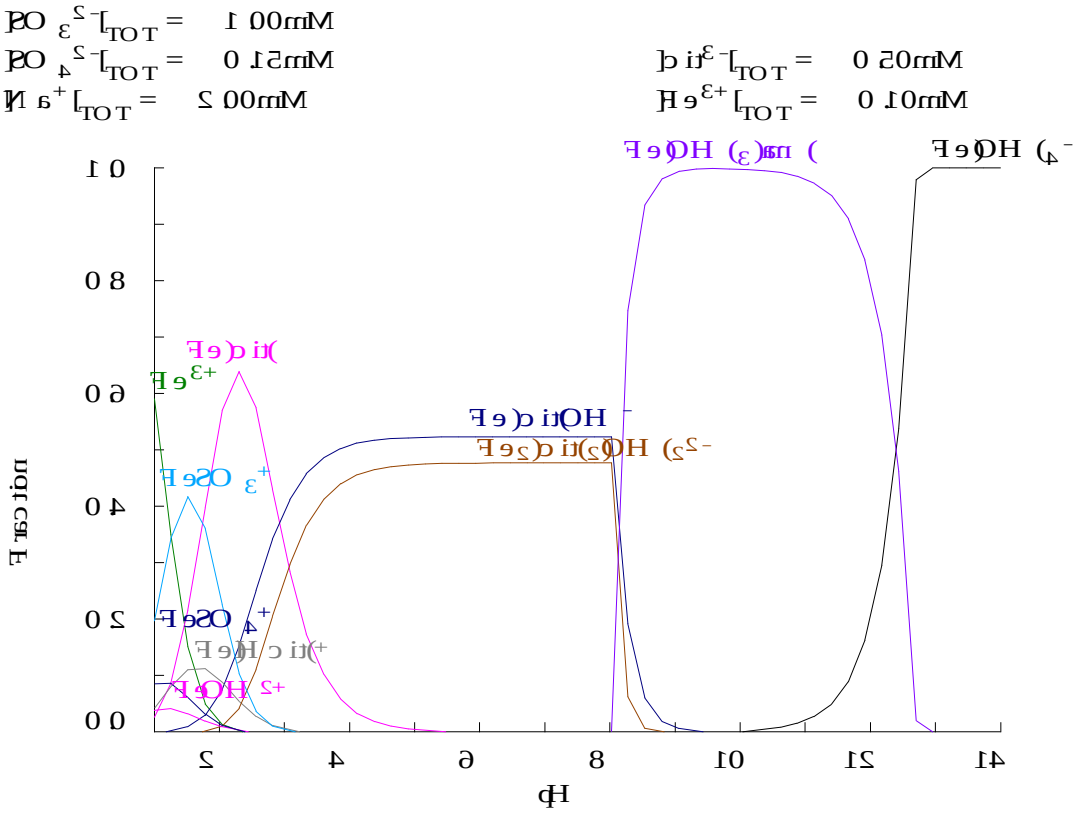

Figure S35. Fe(III) species distribution in Fe(III)-Cit-S(IV) system.

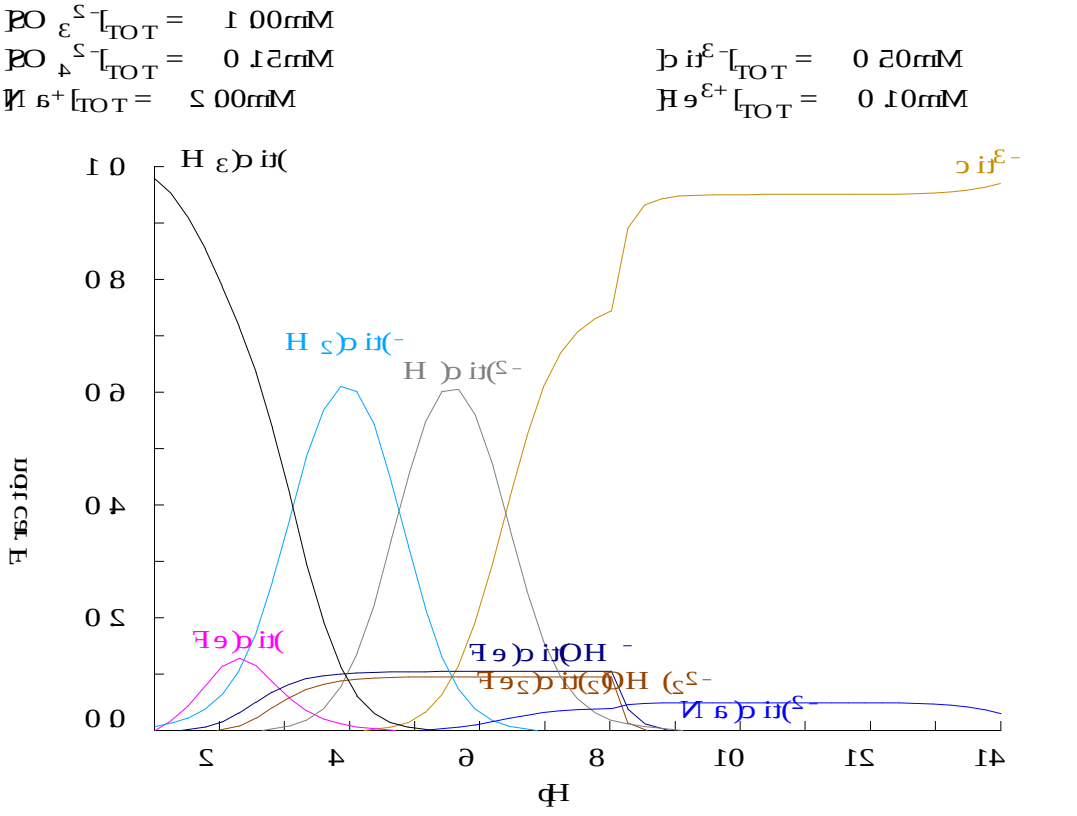

Figure S36. Citrate species distribution in Fe(III)-Cit-S(IV) system.

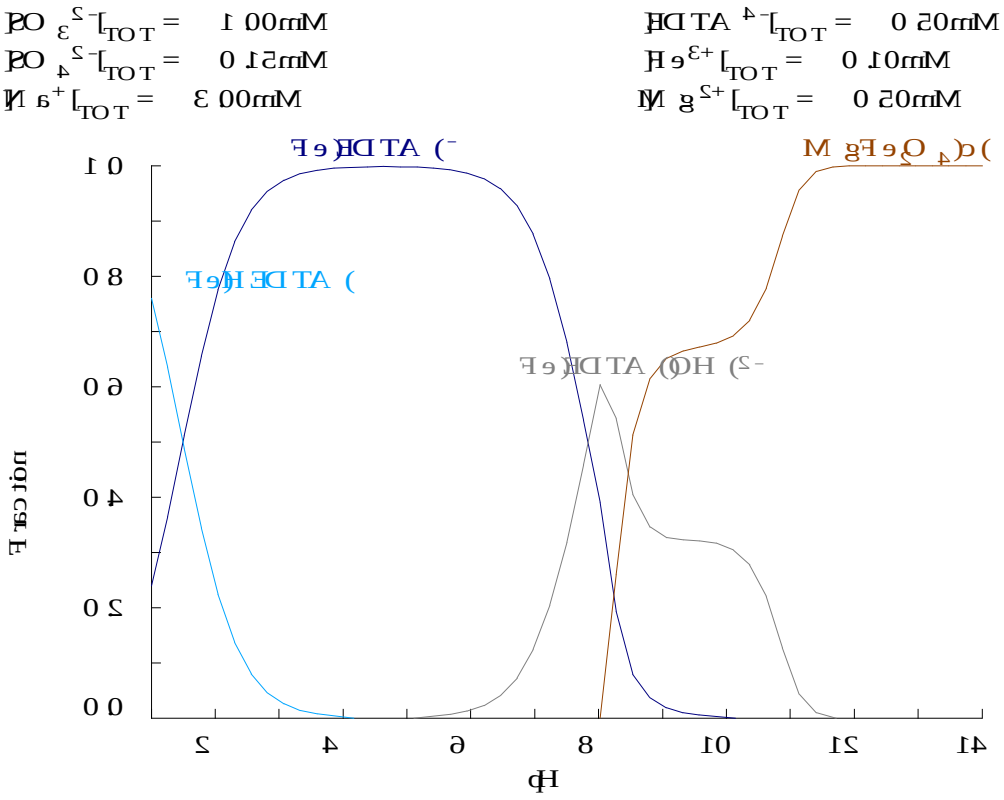

Figure S37. Fe(III) species distribution in Fe (III)-EDTA-S(IV) system.

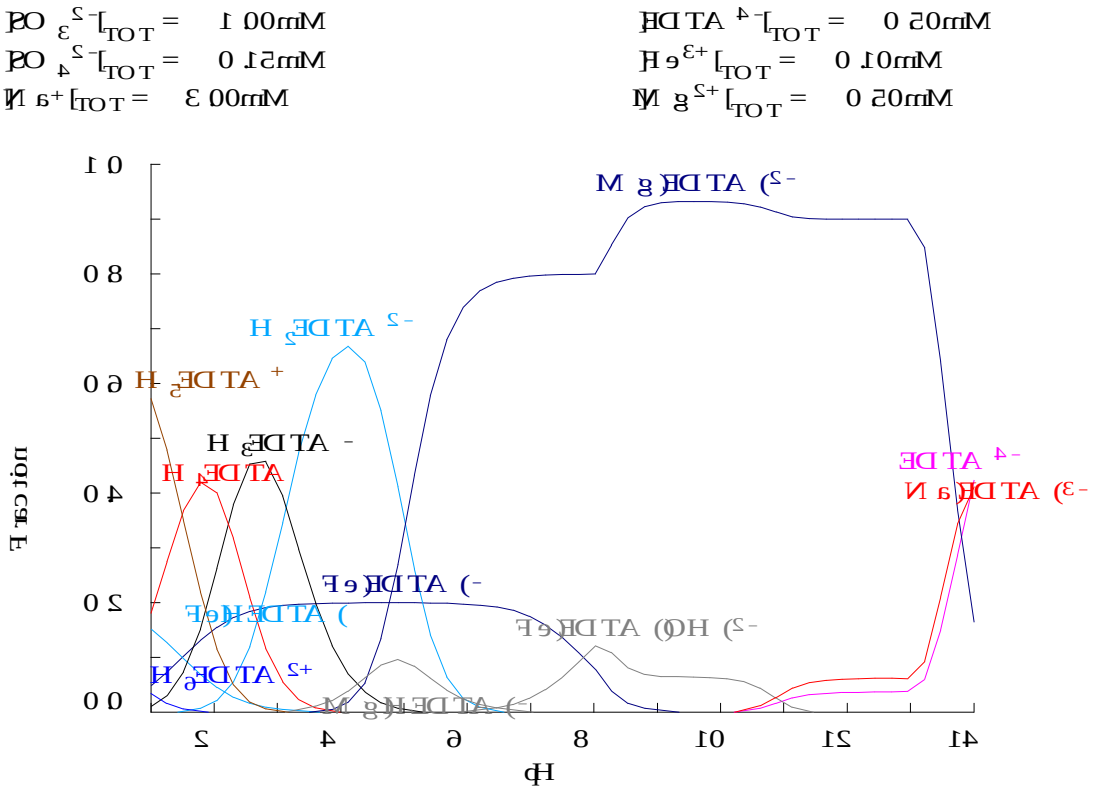

Figure S38. EDTA species distribution in Fe(III)-EDTA-S(IV) system.

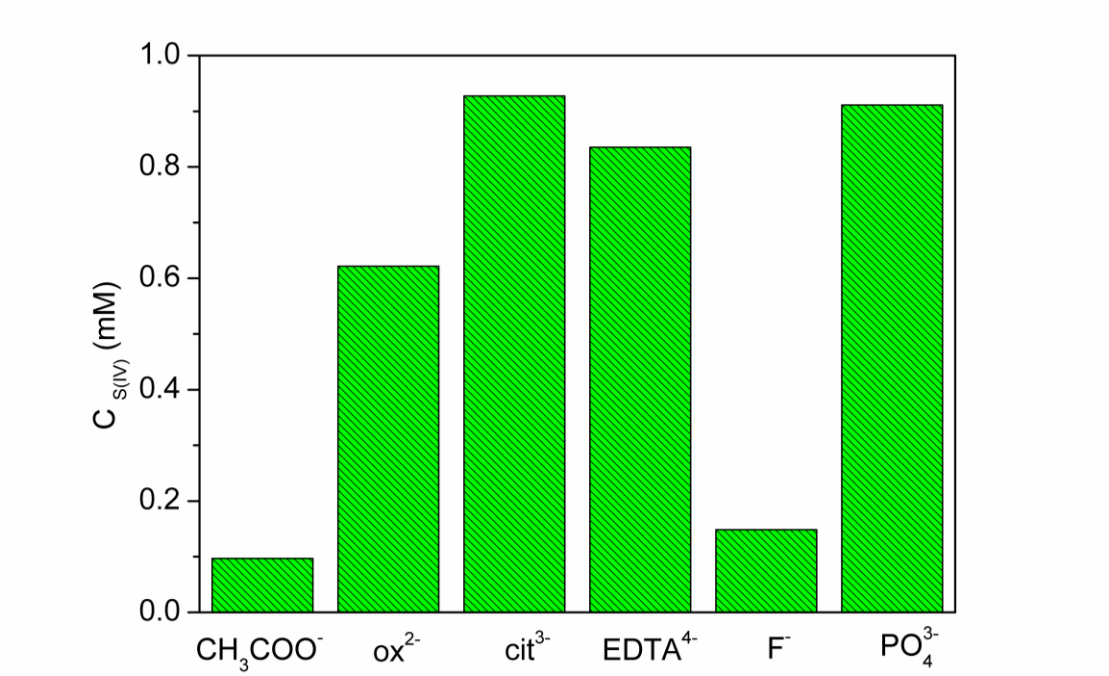

Figure S39. The dosages of S(IV) after 2,4,6-TCP degradation for 30 min when Fe(III)-complexing ligands added into the photo-sulfite system. Conditions: $[2,4,6\text{-TCP}]_0$ = 10 mg/L, $[Fe_2(SO_4)_3]_0$ = 0.05 mM, $[CH_3COONa]_0 = [Ox]_0 = [Cit]_0 = [EDTA]_0 = [NH_4F]_0 = [H_3PO_4]_0$ = 0.5 mM, $[Na_2SO_3]_0$ = 1 mM, pH_{ini} = 4.

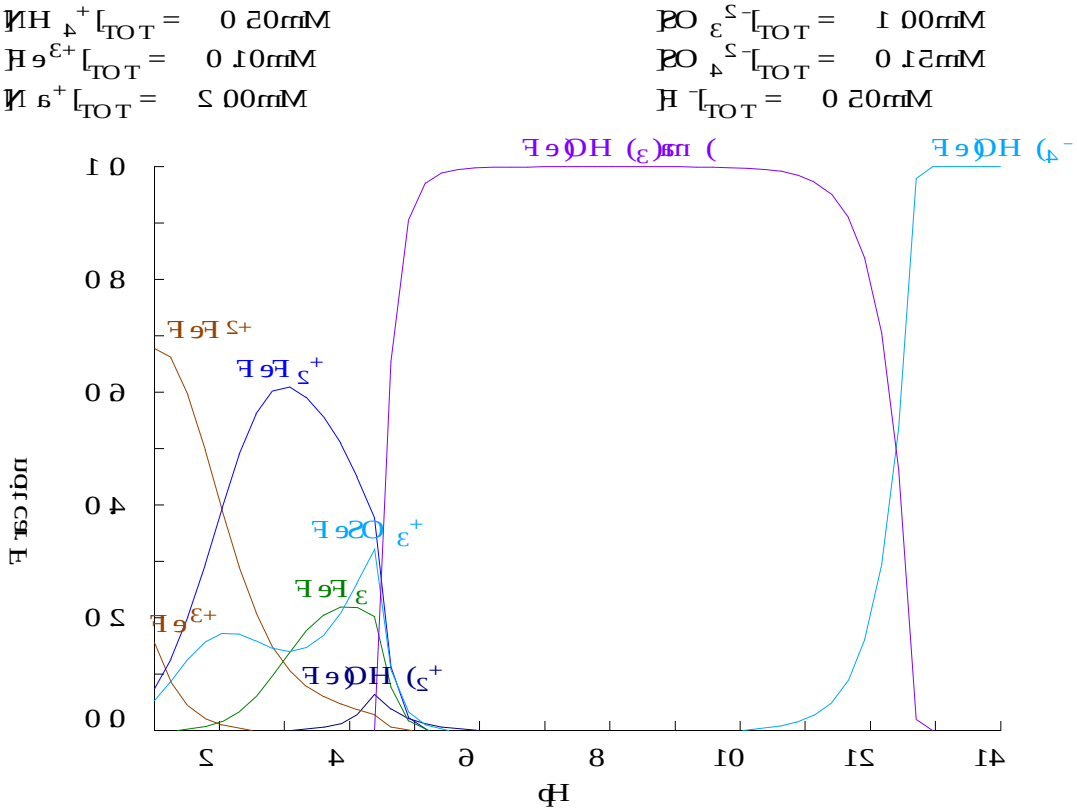

Figure S40. Fe(III) species distribution in Fe (III)-NH_4F-S(IV) system.

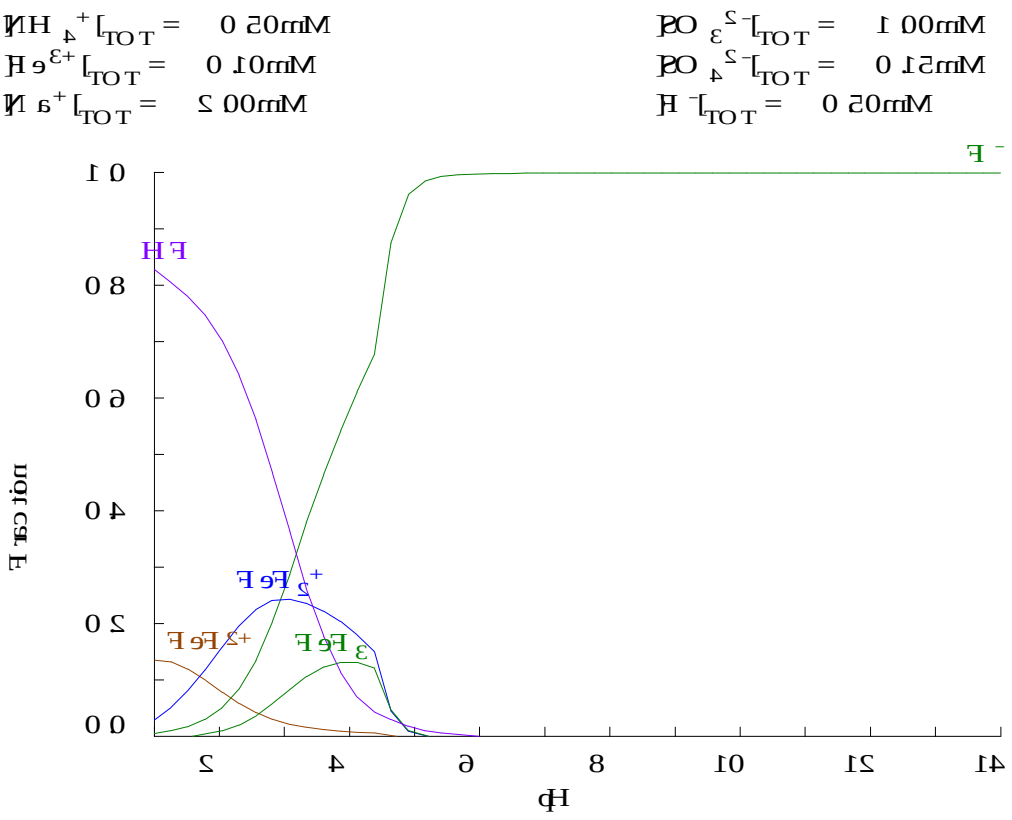

Figure S41. F species distribution in Fe(III)-NH_4F-S(IV) system.

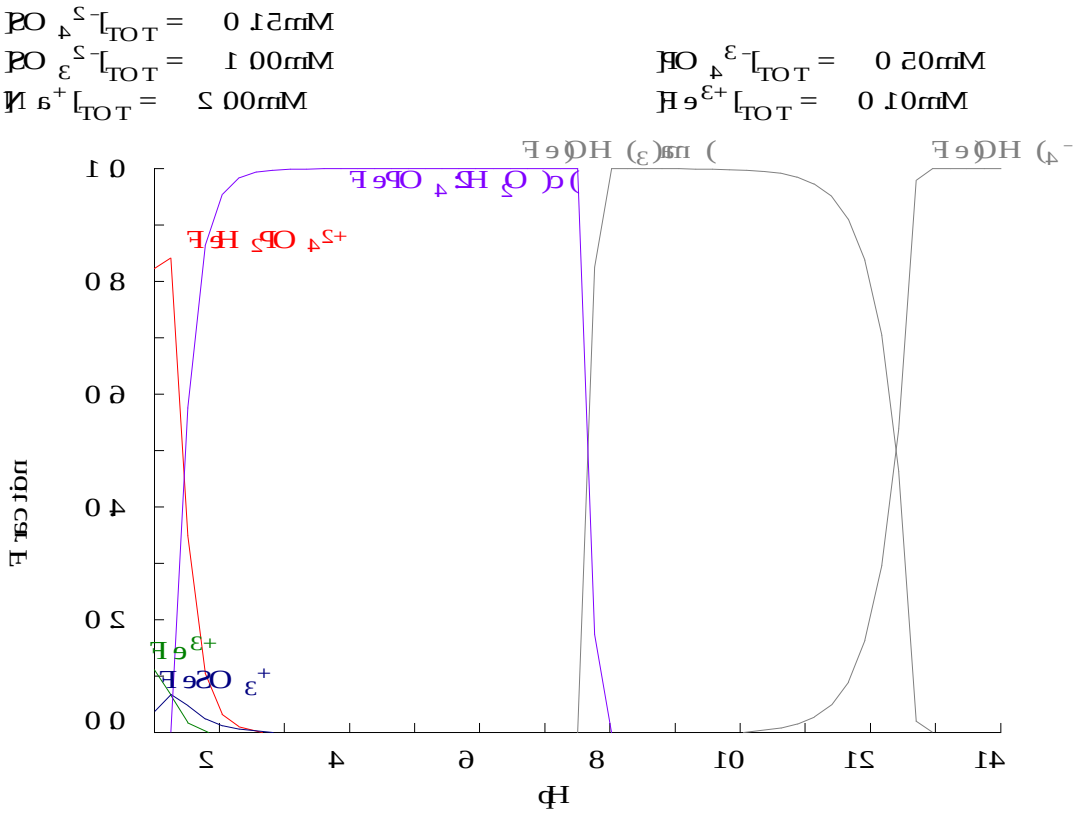

Figure S42. Fe (III) species distribution in Fe (III)-H_3PO_4-S(IV) system.

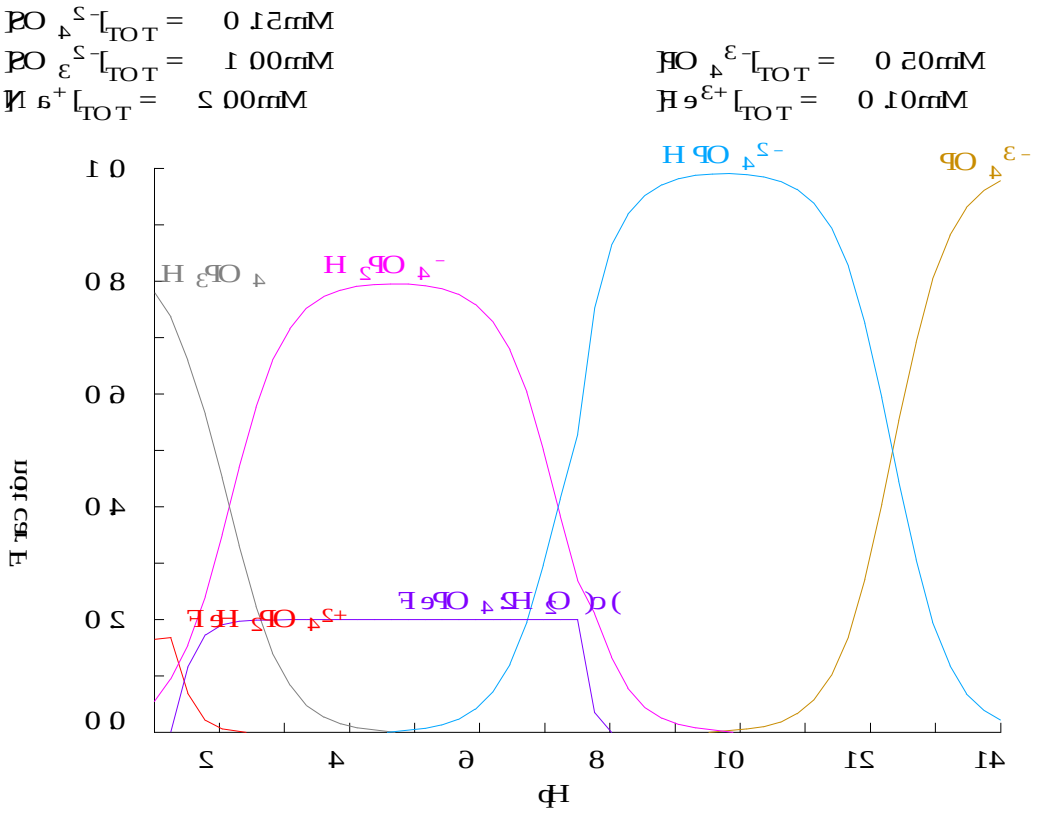

Figure S43. Phosphate species distribution in Fe(III)-H_3PO_4-S(IV) system.

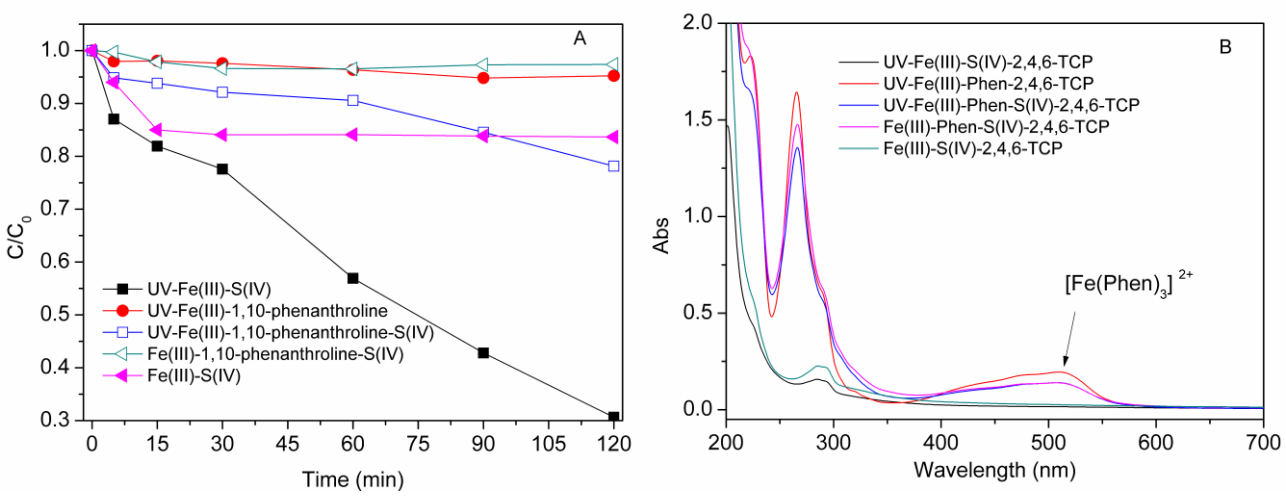

Figure S44. The effect of Phen on the degradation of 2,4,6-TCP (A) and the UV-visible spectrum of the degradation of 2,4,6-TCP after 120 min in different systems (B). Conditions: $[2,4,6\text{-TCP}]_0$ = 10 mg/L, $[Fe_2(SO_4)_3]_0$ = 0.05 mM, $[Phen]_0$ = 0.5 mM, $[Na_2SO_3]_0$ = 1 mM, pH_{ini} = 4.

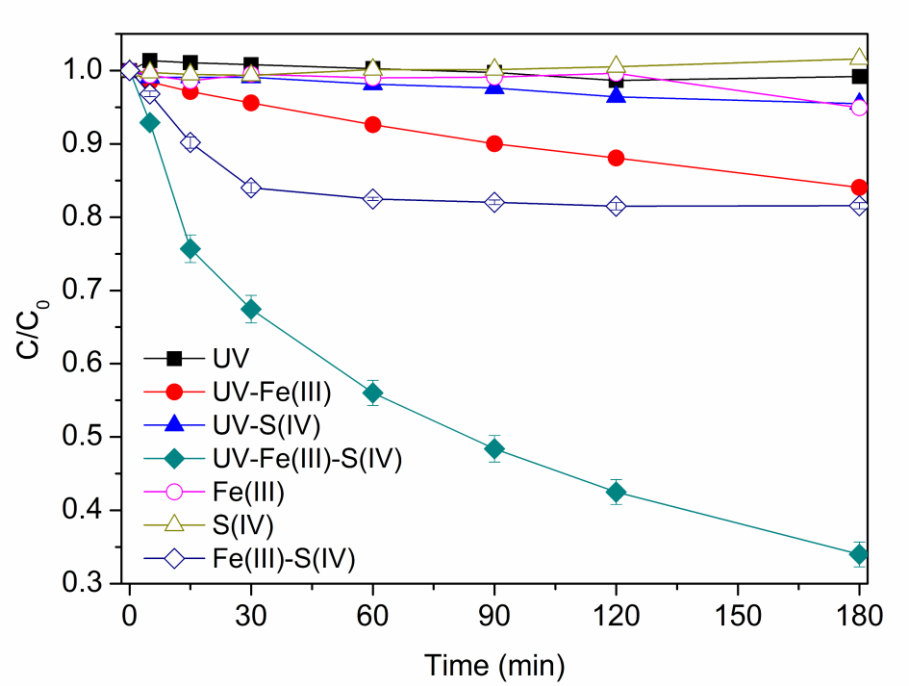

Figure S45. Decoloration of MO under varying experimental conditions. $[MO]_0$ = 10 mg/L, $[Fe_2(SO_4)_3]_0$ = 0.05 mM, $[Na_2SO_3]_0$ = 1 mM, pH_{ini} = 4.

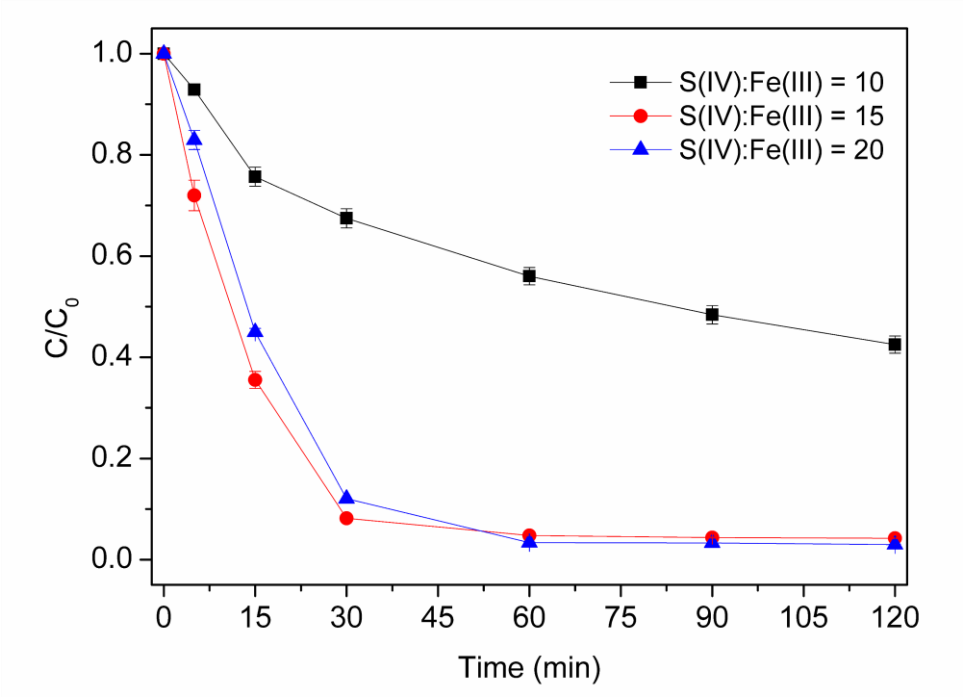

Figure S46. The degradation of MO under varying initial dosages ratio of S(IV): Fe (III) conditions in the photo-sulfite system. Conditions: $[MO]_0$ = 10 mg/L, $[Fe_2(SO_4)_3]_0$ = 0.05 mM , pH_{ini} = 4.

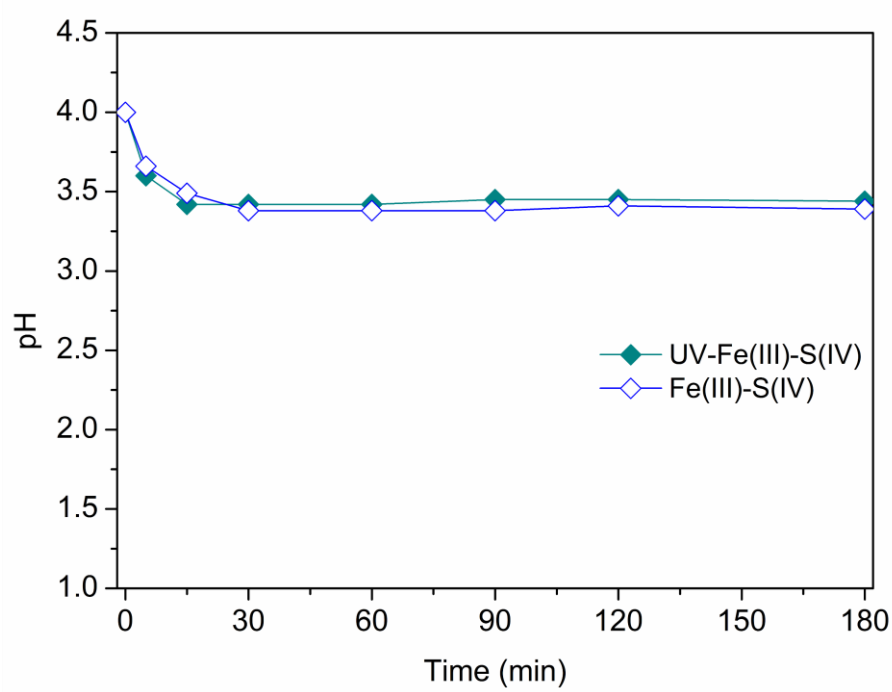

Figure S47. The changes of pH during the degradation of MO in the UV-Fe(III)-S(IV) and Fe(III)-S(IV) systems. Conditions: $[MO]_0$ = 10 mg/L, $[Fe_2(SO_4)_3]_0$ = 0.05 mM, $[Na_2SO_3]_0$ = 1 mM, pH_{ini} = 4.

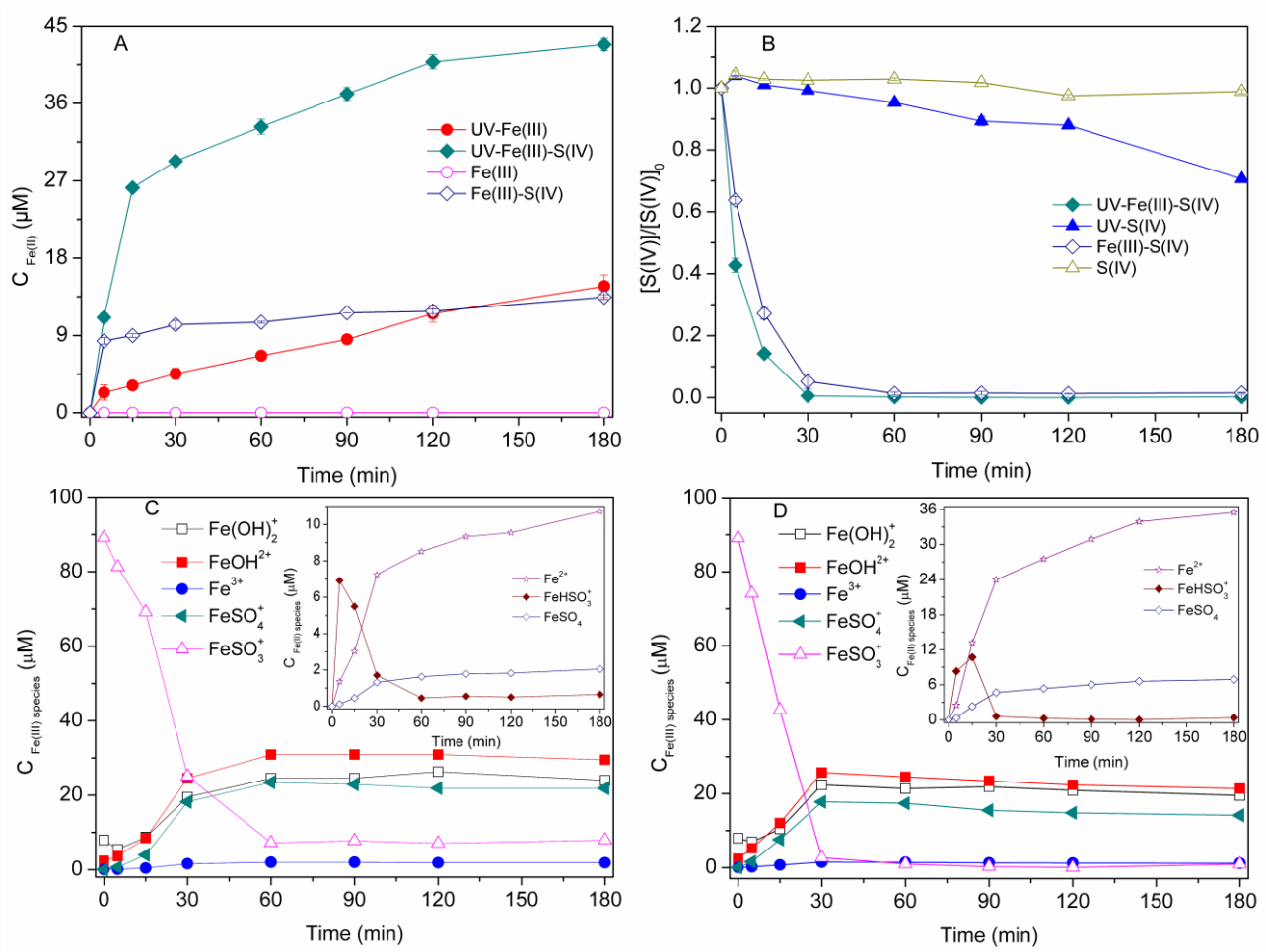

Figure S48. The variations of Fe(II) concentration (A), S(IV) conversion (B), Fe speciation during the MO degradation in Fe(III)-S(IV) system (C) and UV-Fe(III)-S(IV) system (D). Conditions: $[MO]_0$ = 10 mg/L, $[Fe_2(SO_4)_3]_0$ = 0.05 mM, $[Na_2SO_3]_0$ = 1 mM, pH_{ini} = 4. *Inset*: plots of Fe(II) speciation variation versus reaction time during the MO degradation in the Fe(III)-S(IV) system (C) and UV-Fe(III)-S(IV) system (D). *Note*: For determination of Fe(II) and S(IV), all absorbance readings were corrected by subtraction of MO absorbance at 510nm and 412 nm, respectively.

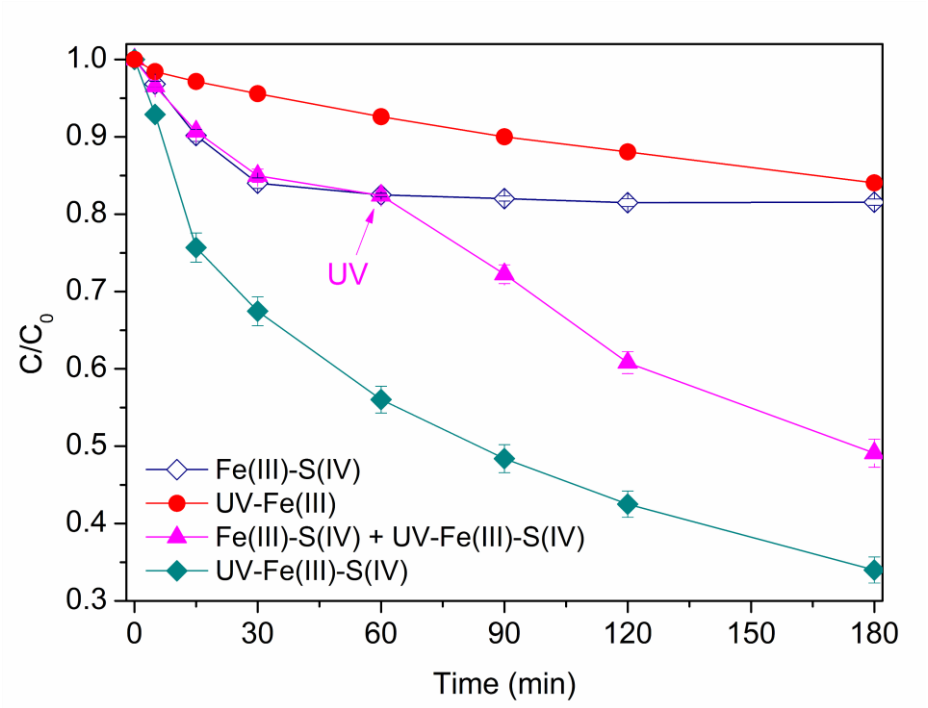

Figure S49. The decoloration of MO when UV irradiation introduction into Fe (III)-S(IV) after 60 min. Conditions: $[MO]_0$ = 10 mg/L, $[Fe_2(SO_4)_3]_0$ = 0.05 mM, $[Na_2SO_3]_0$ = 1 mM, pH_{ini} = 4.

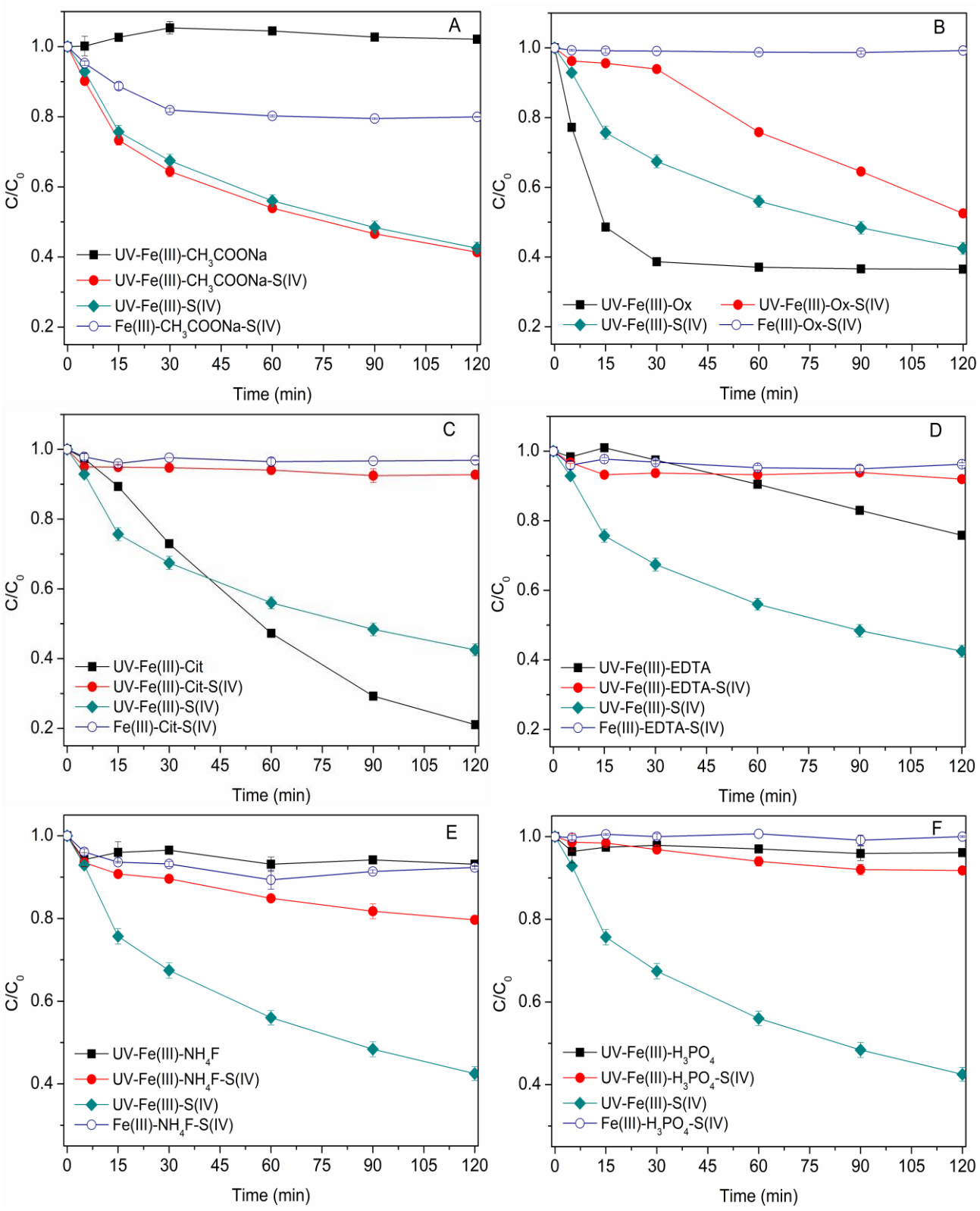

Figure S50. The effects of Fe(III) complexation on the decoloration of MO. Conditions: $[MO]_0$ = 10 mg/L, $[Fe_2(SO_4)_3]_0$ = 0.05 mM, $[CH_3COONa]_0$ = $[Ox]_0$ = $[Cit]_0$ = $[EDTA]_0$ = $[NH_4F]_0$ = $[H_3PO_4]_0$ = 0.5 mM, $[Na_2SO_3]_0$ = 1 mM, pH_{ini} = 4.

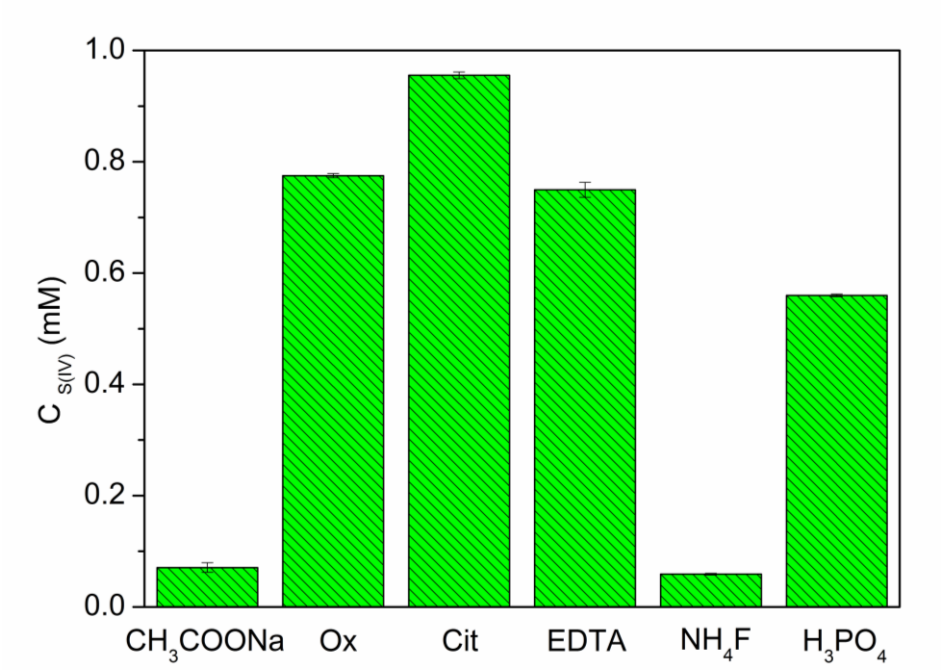

Figure S51. The dosages of S(IV) after MO degradation for 30 min when Fe(III)-complexing ligands added into the photo-sulfite system. Conditions: $[MO]_0$ = 10 mg/L, $[Fe_2(SO_4)_3]_0$ = 0.05 mM, $[CH_3COONa]_0 = [Ox]_0 = [Cit]_0 = [EDTA]_0 = [NH_4F]_0 = [H_3PO_4]_0$ = 0.5 mM, $[Na_2SO_3]_0$ = 1 mM, pH_{ini} = 4.

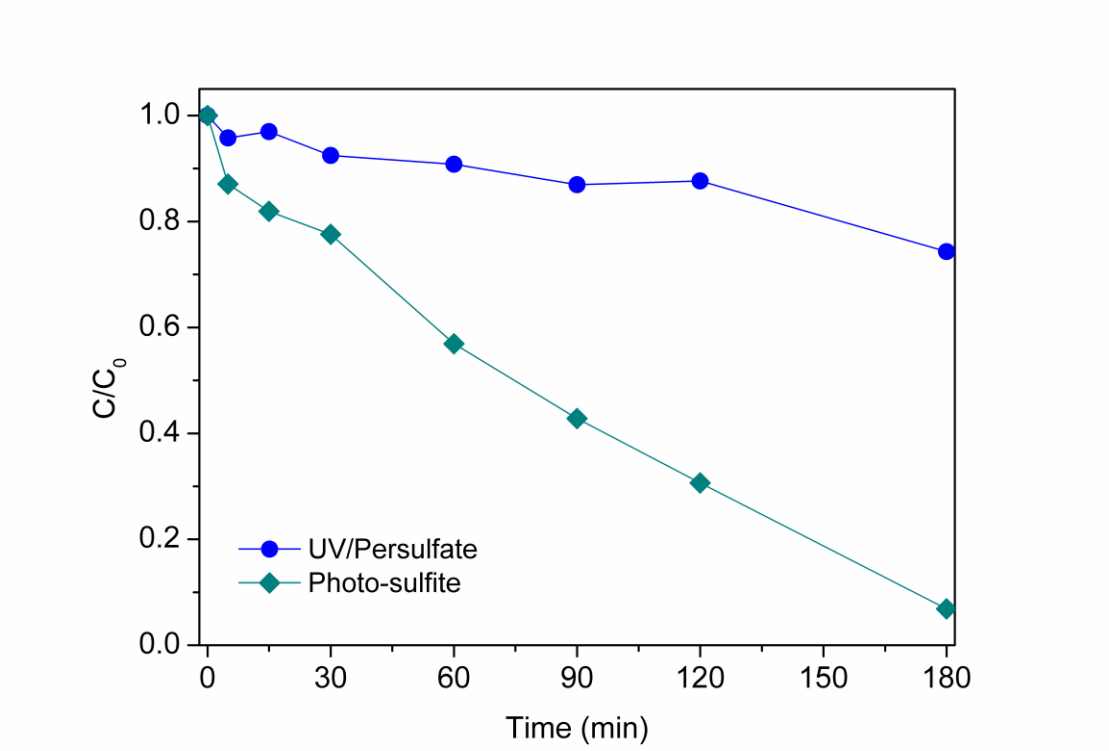

Figure S52. Degradation of 2,4,6-TCP in the photo-sulfite and UV/persulfate systems. Conditions: $[2,4,6\text{-TCP}]_0$ = 10 mg/L, $[Fe_2(SO_4)_3]_0$ = 0.05 mM, $[Na_2SO_3]_0 = [K_2S_2O_8]_0$= 1 mM, pH_{ini} = 4.